Bulk photovoltaic effects in the presence of a static electric field

Benjamin M. Fregoso

Phys. Rev. B **100**, 064301 — Published 2 August 2019

DOI: 10.1103/PhysRevB.100.064301

Bulk photovoltaic effects in the presence of a static electric field

Benjamin M. Fregoso
Department of Physics, Kent State University, Kent, Ohio, 44242, USA

This paper presents a study of dc photocurrents in biased insulators to the third order in the electric field. We find three photocurrents which are characterized by physical divergences of the third-order free-electron polarization susceptibility. In the absence of momentum relaxation and saturation effects, these dc photocurrents grow as t^n $(n = 2, 1, 0)$ with illumination time. The photocurrents are dubbed *jerk*, third-order injection, and third-order shift current, respectively, and are generalizations of the second-order injection and shift currents of the bulk photovoltaic effect. We show that the injection, shift, and jerk currents admit simple physical interpretations in terms of semiclassical wavepacket dynamics and the concept of intraband current. Experimental signatures and extensions to higher-order susceptibilities are also discussed.

I. INTRODUCTION AND MAIN RESULTS

Electrons in crystals can exhibit fascinating dynamics in the presence of external electric and magnetic fields. In metals, the anomalous Hall effect in metallic ferromagnets[1,2] or the chiral anomaly in Weyl semimetals[3,4] are two examples. Insulators, despite lacking a Fermi surface, can also exhibit nontrivial carrier dynamics such as injection and shift currents. Generically referred as bulk photovoltaic effect (BPVE), the injection and shift currents are dc photocurrents in irradiated homogeneous insulators or semiconductors that lack inversion symmetry.

The peculiar nature of the BPVE was first noticed by its photocurrent dependence on light polarization, its dependence on the intensity of light, and by its large open-circuit photovoltages. This led to the first successful phenomenological theory of both components of the BPVE, namely, the injection and shift current.[5–7] Later, quantum kinetic theory was used to find explicit microscopic expressions for the response tensors[5,8]. The BPVE has been extensively studied since the 1960s in ferroelectrics in the context of photovoltaic applications. More recently, the BPVE has attracted attention for its promise in novel optoelectric applications;[9,10] specifically in two-dimensional (2D) ferroelectrics.[11–13]

In the injection current, also called circular photogalvanic effect (CPGE), the lack of inversion symmetry can be manifested in two scenarios. In the first scenario, photoexcited carriers relax momentum asymmetrically into $\pm\mathbf{k}$ directions via collisions with other electrons, phonons or impurities. This leads to a polar distribution and a net current[5–7]. In the second scenario, light pumps carriers into velocity-carrying states asymmetrically at $\pm\mathbf{k}$ points in the Brillouin zone (BZ) leading to a polar distribution and a net current[5,14]. In both scenarios, the key point is that the rate of pumping into or out of current-carrying states at time-reversed directions is asymmetrical. Within a simple relaxation time approximation, the steady state injection current in both cases is proportional to the first power of the relaxation time constant and vanishes for linearly polarized light.

The shift current, on the other hand, has a distinct microscopic origin which is not completely understood. It is known that shift current processes involve the coherent transfer of charge across a unit cell. This happen because materials that lack inversion symmetry have the centers of charge in the valence and conduction bands spatially separated. The shift current vanishes for circular polarization of light and decays in the time scale of the quantum coherence of the solid.

The injection or shift current (or both) has been reported in ferroelectric materials[9,11,15–23], GaAs[24,25], CdSe[26,27], CdS[27], quantum wells[28,29], RhSi[30], $Bi_{12}GeO_{20}$[31], and others as reported previously.[5,32–34]

Following Sipe and coworkers[14], BPVE response tensors can be derived from the perspective of divergent polarization susceptibilities. In this approach, the inversion symmetry breaking is encoded in light-matter interactions and not on momentum relaxation processes; the latter are included phenomenologically a *posteriori*. For not too large electric fields, the insulator's response to an external electric field is described perturbatively by susceptibilities χ_n as

$$\mathbf{P} = \mathbf{P}_0 + \chi_1\mathbf{E} + \chi_2\mathbf{E}^2 + \chi_3\mathbf{E}^3 + \cdots, \tag{1}$$

where $\mathbf{P}_0$ is the electric polarization in the absence of an external electric field,[35,36] χ_1 is the linear susceptibility, and $\chi_2, \chi_3, ...$ are nonlinear susceptibilities.[37]

The electric polarization in insulators is commonly thought to be determined by the off-diagonal elements of the density matrix because these elements describe the displacement of charge from its equilibrium position in the presence of an electric field. Intraband processes, however, have been shown to be important.[39,42,43] Among other things they cure unphysical divergences in susceptibilities in the dc limit by incorporating the fact that the intraband motion of Bloch electrons cannot accelerate indefinitely in insulators[39,42]. Importantly, when intraband and interband processes are taken into account on an equal footing divergent susceptibilities represent real photocurrents.

Consider, for example, the dc divergences of χ_2. If we denote the amplitude of the electric field by $E^b = \sum_\beta E^b_\beta e^{-i\omega_\beta t}$, the polarization to second order is

TABLE I. Summary of bulk photovoltaic effects (BPVEs) obtained from divergences of free electric polarization susceptibilities. The 2nd injection and shift current are derived from singularities in χ_2 at zero frequency. The BPVEs can be classified by their dependence on illumination time in the absence of momentum relaxation and saturation effects, e.g., η_2, η_3 and η_4 are called injection current responses and similarly σ_2, σ_3 are called shift currents responses. We write susceptibilities as, $\chi_n^{abc\cdots}(-\omega_\Sigma,\omega_\beta,\omega_\sigma,...)$ where $b,c...$ are Cartesian indices, $\omega_\beta,\omega_\sigma,...$ are frequency components, and $\omega_\Sigma=\omega_\beta+\omega_\sigma+...$ frequency sums[38]. $[X,Y]$ ($\{X,Y\}$) indicate commutation (anticommutation) with respect to b,c indices only. Other conventions are explained in Sec. II.

BPVE	Symbol	Expression	Time dependence $\sim t^\alpha$	Origin	Ref.
Injection	η_2^{abc}	$\frac{\pi e^3}{2\hbar^2 V}\sum_{nm\mathbf{k}} f_{mn}\ \omega_{nm;a}[r^b_{nm},r^c_{mn}]\delta(\omega_{nm}-\omega)$	1	$\chi_2(0,\omega,-\omega)\ \to\ \infty$	39
Shift	σ_2^{abc}	$\frac{i\pi e^3}{2\hbar^2 V}\sum_{nm\mathbf{k}} f_{mn}\{r^c_{nm;a},r^b_{mn}\}\delta(\omega_{nm}-\omega)$	0		39
Jerk	ι_3^{abcd}	$\frac{\pi e^4}{3\hbar^3 V}\sum_{nm\mathbf{k}} f_{mn}\left[2\omega_{nm;ad}r^b_{nm}r^c_{mn}+\omega_{nm;a}(r^b_{nm}r^c_{mn})_{;d}\right]\delta(\omega_{nm}-\omega)$	2	$\chi_3(0,\omega,-\omega,0)\ \to\ \infty$	40
Injection	η_3	Eq. 122	1		present
Shift	σ_3	Eq. 140	0		present
Injection	ν_3	Eq. 7	1	$\chi_3(0,-2\omega,\omega,\omega)\ \to\ \infty$	41
Shift	σ_3	Eq. 8	0		41
Snap	ς_4	Eq. 161	3	$\chi_4(0,\omega,-\omega,0,0)\ \to\ \infty$	present
Jerk	ι_4		2		
Injection	η_4		1		
shift	σ_4		0		
Any	a_n	$\frac{1}{2\pi i}\oint_{\lvert z\rvert=\rho} dz\frac{\chi_n}{z^{l+1}}$, $z=-i\omega_\Sigma$, $\rho\to 0$, $l=-n,\cdots,-1$, Eq. 169	$\alpha=n-1,...,0$	$\chi_n(\omega_\Sigma,\omega_\beta,\omega_\sigma,...)\ \to\ \infty$, $\omega_\Sigma=\omega_\beta+\omega_\sigma+\cdots\to 0$	present

$$P^{a(2)}=\sum_{b\beta c\sigma}\chi_2^{abc}(-\omega_\Sigma,\omega_\beta,\omega_\sigma)E^b_\beta E^c_\sigma e^{-i\omega_\Sigma t}, \tag{2}$$

and oscillates with frequency $\omega_\Sigma=\omega_\beta+\omega_\sigma$ in the long-time limit. It can be shown that the intraband, χ_{2i}, contribution to χ_2

$$\chi_2=\chi_{2i}+\chi_{2e}, \tag{3}$$

can be expanded in powers of ω_Σ as[14,39]

$$(-i\omega_\Sigma)^2\chi_{2i}=\eta_2+(-i\omega_\Sigma)\sigma_2+\cdots. \tag{4}$$

In can be shown that the interband component χ_{2e} is regular as $\omega_\Sigma\to 0$. Together with the Maxwell equation

$$\frac{d\mathbf{P}}{dt}=\mathbf{J}, \tag{5}$$

and assuming a monocromatic optical field, Eq. 4 implies η_2 and σ_2 are response functions of the nonlinear currents

$$\frac{d}{dt}J^{a(2)}_{inj}\equiv 2\sum_{bc}\eta_2^{abc}(0,\omega,-\omega)E^b(\omega)E^c(-\omega), \tag{6}$$

$$J^{a(2)}_{sh}\equiv 2\sum_{bc}\sigma_2^{abc}(0,\omega,-\omega)E^b(\omega)E^c(-\omega). \tag{7}$$

η_2 and σ_2 are the standard injection and shift current response functions derived from the susceptibility approach.[14] Importantly, they vanish for frequencies smaller than the energy gap (they are 'resonant'). The dots in Eq. 4 are associated with the (nonresonant) rectification currents.[44,45]. In the absence of momentum relaxation and saturation effects the injection and shift currents grow with illumination time as

$$|J^{a(2)}_{inj}|\propto\eta_2 t \tag{8}$$

$$|J^{a(2)}_{sh}|\propto\sigma_2. \tag{9}$$

In this article we show how the injection and shift currents are modified by the presence of a static field from the perspective of the physical dc divergences of the free third order electric polarization susceptibility χ_3. Biased irradiated semiconductors of this kind have been extensively studied numerically using the semiclassical Boltzmann equation.[46] As shown below, this approach misses some important quantum effects which are recovered in the susceptibility approach.

The third order polarization

$$P^{a(3)} = \sum_{b\beta c\sigma d\delta} \chi_3^{abcd}(-\omega_\Sigma, \omega_\beta, \omega_\sigma, \omega_\delta) E_\beta^b E_\sigma^c E_\delta^d e^{-i\omega_\Sigma t}, \tag{10}$$

oscillates with frequency $\omega_\Sigma = \omega_\beta + \omega_\sigma + \omega_\delta$ in the long-time limit. We show that the intraband part, χ_{3i}, of $\chi_3 = \chi_{3i} + \chi_{3e}$ admits the Taylor expansion

$$(-i\omega_\Sigma)^3 \chi_{3i} = \iota_3 + (-i\omega_\Sigma)\eta_3 + (-i\omega_\Sigma)^2 \sigma_3 + \cdots, \tag{11}$$

or alternatively the Laurent series

$$\chi_{3i} = \frac{\iota_3}{z^3} + \frac{\eta_3}{z^2} + \frac{\sigma_3}{z} + \cdots, \tag{12}$$

where $z = -i\omega_\Sigma$ and ι_3, η_3, σ_3 are (resonant) residues. Clearly, χ_{3i} diverges in the dc limit ($\omega_\Sigma = 0$) and similar to η_2 and σ_2, ι_3, η_3 and σ_3 represent response functions of nonlinear currents

$$\frac{d^2}{dt^2} J_{jerk}^{a(3)} \equiv 6 \sum_{bcd} \iota_3^{abcd}(0, \omega, -\omega, 0) E^b(\omega) E^c(-\omega) E_0^d \tag{13}$$

$$\frac{d}{dt} J_{inj}^{a(3)} \equiv 6 \sum_{bcd} \eta_3^{abcd}(0, \omega, -\omega, 0) E^b(\omega) E^c(-\omega) E_0^d \tag{14}$$

$$J_{sh}^{a(3)} \equiv 6 \sum_{bcd} \sigma_3^{abcd}(0, \omega, -\omega, 0) E^b(\omega) E^c(-\omega) E_0^d. \tag{15}$$

The difference is that a static field (zero frequency) is taken into account in addition to a monochromatic optical field. In the absence of momentum relaxation and saturation effects the currents vary as t^2, t, t^0 with illumination time and we dub them jerk, 3rd-order injection current and 3rd-order shift current, respectively. The dots in Eq. (12) represent regular terms associated with rectification currents.

Since χ_{3e} is regular in the dc limit one can write the same expansion as in Eq. (12) for both χ_{3i} and χ_3. Similarly, the third order photoconductivity which is defined by

$$J^{a(3)} \equiv \sum_{b\beta c\sigma d\delta} \sigma^{abcd(3)}(-\omega_\Sigma, \omega_\beta, \omega_\sigma, \omega_\delta) E_\beta^b E_\sigma^c E_\delta^d e^{-i\omega_\Sigma t}, \tag{16}$$

admits the expansion

$$\sigma^{(3)} = \frac{\iota_3}{z^2} + \frac{\eta_3}{z} + \sigma_3 + \cdots. \tag{17}$$

The macroscopic current dynamics in a sample involves not only the above generation processes but also the subsequent evolution of charge distribution in the sample.

In the presence of dissipation, the dc divergences will be cut-off by a momentum relaxation time scale, just as the dc divergence of metals in the Drude model is cut-off by a momentum relaxation time. In the BPVE, we expect two relevant relaxation time scales. One is the relaxation time scale of the diagonal elements of the density matrix, τ_1, which ι_3, η_3, and η_2 depend on. This could be of the order of 100 fs or longer in clean semiconductors[47]. The second is the relaxation time scale of the off-diagonal elements of the density matrix, τ_2, which σ_3 and σ_2 depend on. Typically, we expect $\tau_2 < \tau_1$, but a recent experiment found τ_2 to be as large as 250 fs.[25] For weakly disordered semiconductors, the conductivity at $\omega_\Sigma = 0$ becomes

$$\sigma^{(3)} = \tau_1^2 \iota_3 + \tau_1 \eta_3 + \sigma_3. \tag{18}$$

Note that $\sigma^{(3)}$ can also be viewed as the photoconductivity, i.e., the light-dependent correction to the dc conductivity.[5]

We can generalize the above results to any power in the electric fields. In general, with each additional power in the electric field, χ_{ni} has an additional frequency factor in the denominator. This means that the dc singularities of χ_{ni} are, at most, of the order n. We can show that the nth order $z = 0$ singularities of χ_n ($n \geq 2$), represent photocurrents which vary as t^n in the absence of momentum relaxation and saturation effects. This occurs when all but two of the external frequencies are zero. In addition, there is a hierarchy of higher order shift, injection,..., currents which are represented by $z = 0$ singularities of order $1, 2, 3, ..n$ of χ_n. Formally χ_n can be expanded as

$$\chi_n = \sum_{l=-n}^{\infty} a_l z^l, \tag{19}$$

where $a_l = 0$ for frequencies less than the gap and hence the residues are

$$a_l = \frac{1}{2\pi i} \oint_{|z|=\rho} \frac{\chi_n \, dz}{z^{l+1}}. \tag{20}$$

The poles of χ_n may be of lower order than n when the optical field is not monocromatic; see, for example, the 4th row in Table I where the field's frequencies are ω and 2ω.

Importantly, we give simple physical arguments to explain the microscopic processes involved in ι_3, η_3, σ_3 and σ_2 and provide explicit expressions in terms of material parameters amenable for first principles computations. To have a sense of the magnitude of these currents, we calculate them in single-layer GeS using a two-dimensinal (2D) tight-binding model. In particular we give specific signatures of these currents for ultrafast THz experiments, see Table II.

The article is organized as follows. In Sec. II we describe the conventions used in this paper. In Sec. IV, III,

and V we introduce the Hamiltonian, polarization, and current operators. In Sec. V A we revisit the calculation of the intraband current following Sipe and Shkrebtii.[14]. In Sec. VII we rederive the expressions for the injection and shift current responses giving simple physical interpretations based on semiclassical wavepackets dynamics in electric fields. We then study the physical divergences of χ_3 at zero frequency in Sec. IX, X, and XI. The jerk current has been presented previously and is included here only for completeness[40]. BPVEs arising from singularities of χ_n ($n > 3$) are discussed in Sec. XII A. Experimental signatures in single-layer GeS are summarized in Sec. XIII. A summary of the BPVEs is presented in Table I. Details of the derivations are given in the appendices.

II. NOTATION

To keep the notation under control we often omit the independent variables such as time, real space position, or crystal momentum, specially in expressions which are diagonal in these variables.

We use the standard notation for the nth electric polarization susceptibility,[38] $\chi_n^{abc\cdots}(-\omega_\Sigma\omega_\beta,\omega_\sigma,...)$, where $\omega_\beta,\omega_\sigma,...$ label external frequency components, $abc,...$ label Cartesian components, and $\omega_\Sigma = \omega_\beta + \omega_\sigma + ...$ the frequency sum. We often write $\chi_n^{abc\cdots}$ or simply χ_n for brevity absorbing a free permittivity factor ϵ_0 into the susceptibility.

We adopt a semicolon and subscript, '$;a$', to mean a covariant derivative with respect to crystal momenta with respect to Cartesian component $a = x, y, z$. Unless otherwise specified we contract the spinor index, e.g., $n\alpha \to n$ in all expressions. A hat on a Hamiltonian, polarization, and current indicates an operator and a lack of a hat means a quantum mechanical average. We do not use hats on the creation or annihilation operators or on the position operator. A bold font indicates a vector or spinor.

To distinguish the injection current derived from η_3 from that of η_2 we often call the former 3rd-order injection current and the latter 2nd-order injection current. Similarly, 3rd-order shift current refers to current derived from σ_3. We hope the missing details will become clear from the context.

III. HAMILTONIAN

We start from a Hamiltonian

$$\hat{H}_0 = \int d\mathbf{r}\ \boldsymbol{\psi}^\dagger \left(\frac{\hat{p}^2}{2m} + V(\mathbf{r}) + \mu_B^2 \mathbf{e}\cdot(\hat{\mathbf{p}}\times\boldsymbol{\sigma}) \right) \boldsymbol{\psi} \quad (21)$$

$$+\hat{H}_{int}, \quad (22)$$

describing Bloch electrons with spin-orbit (SO) coupling, where $V(\mathbf{r})$ is the periodic potential of the ions, $\hat{\mathbf{p}} = -i\hbar\boldsymbol{\nabla}_{\mathbf{r}}$ is the momentum operator, $\mathbf{e}(\mathbf{r}) = -\boldsymbol{\nabla}_{\mathbf{r}} V(\mathbf{r})$ is the SO field from the nucleus, and $\mu_B = e\hbar/2mc$ is the Bohr magneton. $\hat{H}_{int}$ contains interactions with other electrons, phonons, and impurities. We assume a mean field theory for this term. Its effect is to renormalize the parameters of the noninteracting theory. Momentum relaxation is incorporated phenomenologically at the end of the calculation. The electron charge is $e = -|e|$. We define the real space spinor field as

$$\boldsymbol{\psi} = \begin{pmatrix} \psi_\uparrow \\ \psi_\downarrow \end{pmatrix}. \quad (23)$$

A classical homogeneous electric field is coupled to the Hamiltonian by minimal substitution, $\hat{\mathbf{p}} \to \hat{\mathbf{p}} - e\mathbf{A}$. After the gauge transformation

$$\tilde{\psi}_\alpha = \psi_\alpha e^{-ie\mathbf{A}\cdot\mathbf{r}/\hbar}, \quad (24)$$

(α is the spinor component) the Hamiltonian for the transformed fields becomes

$$\hat{H}(t) = \hat{H}_0 + \hat{H}_D(t). \quad (25)$$

In what follows we omit the tilde above the transformed fields. $\hat{H}_0$ is given by Eq. (22), and the perturbation has the dipole form

$$\hat{H}_D = -e \int d\mathbf{r}\ \boldsymbol{\psi}^\dagger\ \mathbf{r}\cdot\mathbf{E}\ \boldsymbol{\psi}. \quad (26)$$

The electric field is given by $\mathbf{E} = -\partial\mathbf{A}/\partial t$. The eigenfunctions of H_0 can be chosen to be Bloch wavefunctions $\boldsymbol{\psi}_n^{(\beta)}(\mathbf{kr}) = \mathbf{u}_n^{(\beta)}(\mathbf{kr})e^{-i\mathbf{kr}}$, where $\mathbf{u}_n^{(\beta)}(\mathbf{k},\mathbf{r}+\mathbf{R}) = \mathbf{u}_n^{(\beta)}(\mathbf{k},\mathbf{r})$ has the period of a lattice vector $\mathbf{R}$. $\mathbf{k}$ is the crystal momentum and $\beta = 1, 2$ is the spinor index. The field operators can then be expanded in Bloch states

$$\psi_\alpha(\mathbf{r}) = \sum_{n\beta\mathbf{k}} \psi_{n\alpha}^{(\beta)}(\mathbf{kr}) a_{n\beta}(\mathbf{k}), \quad (27)$$

where $a_{n\beta}^\dagger(\mathbf{k})$ creates a particle in a Bloch state and obeys anticommutation rules $\{a_{n\alpha}^\dagger(\mathbf{k}), a_{m\beta}(\mathbf{k}')\} = \delta_{nm}\delta_{\alpha\beta}\delta_{\mathbf{kk}'}$ ($= \delta_{nm}(2\pi)^3\delta(\mathbf{k}-\mathbf{k}')/V$ in the thermodynamic limit). In this basis, H_0 is diagonal

$$\hat{H}_0 = \sum_{n\beta\mathbf{k}} \hbar\omega_{n\beta} a_{n\beta}^\dagger a_{n\beta}, \quad (28)$$

and $\hbar\omega_{n\beta}(\mathbf{k})$ is the energy of band n and spinor β. The sum over crystal momenta is confined to the Brillouin Zone (BZ). In the thermodynamic limit in d-dimensions the sum becomes $\sum_{\mathbf{k}} \to V\int d^dk/(2\pi)^d$, where V is the volume of the crystal. In what follows we chose the periodic gauge by which Bloch wavefunctions are periodic in reciprocal lattice vectors, $\boldsymbol{\psi}_n^{(\beta)}(\mathbf{k}+\mathbf{G},\mathbf{r}) = \boldsymbol{\psi}_n^{(\beta)}(\mathbf{k},\mathbf{r})$.

IV. POLARIZATION OPERATOR

The many-body polarization operator is well defined in finite systems. It is given by

$$\hat{\mathbf{P}} = \frac{1}{V}\int d\mathbf{r}\ \boldsymbol{\psi}^\dagger\ e\mathbf{r}\ \boldsymbol{\psi}, \tag{29}$$

where $\hat{\mathbf{P}} = e\mathbf{r}/V$ is the one-body polarization operator. Using the polarization operator Eq. 26, the dipole Hamiltonian becomes simply

$$\hat{H}_D = -V\hat{\mathbf{P}}\cdot\mathbf{E}. \tag{30}$$

In periodic systems, H_D is given in terms of Bloch operators $a_n(\mathbf{k})$ as

$$\hat{\mathbf{P}} = \frac{e}{V}\sum_{nm\mathbf{k}\mathbf{k}'}\langle n\mathbf{k}|\mathbf{r}|m\mathbf{k}'\rangle a_n^\dagger(\mathbf{k})a_m(\mathbf{k}'). \tag{31}$$

Because the position operator is unbounded and the Bloch wavefunctions extend to infinity, the matrix elements (restoring spinor indices)

$$\begin{aligned}\langle n\mathbf{k}|\mathbf{r}|m\mathbf{k}'\rangle \to&\langle n\alpha\mathbf{k}|\mathbf{r}|m\beta\mathbf{k}'\rangle\\ =&\int d\mathbf{r}\ \boldsymbol{\psi}_n^{(\alpha)\dagger}(\mathbf{k}\mathbf{r})\mathbf{r}\ \boldsymbol{\psi}_m^{(\beta)}(\mathbf{k}'\mathbf{r}),\end{aligned} \tag{32}$$

are singular. Fortunately, this singularity does not propagate to observables such as the spontaneous polarization[14] if we separate the singularity by the well-known identity[1,48]

$$\begin{aligned}\langle n\mathbf{k}|\mathbf{r}|m\mathbf{k}'\rangle = \delta_{nm}[\delta(\mathbf{k}-\mathbf{k}')\xi_{nn} + i\boldsymbol{\nabla}_{\mathbf{k}}\delta(\mathbf{k}-\mathbf{k}')]+\\ (1-\delta_{nm})\delta(\mathbf{k}-\mathbf{k}')\xi_{nm}.\end{aligned} \tag{33}$$

Here ξ_{nm} are the Berry connections

$$\xi_{nm}\to\xi_{n\alpha m\beta} = \int d\mathbf{r}\ \mathbf{u}_n^{(\alpha)\dagger}\ i\boldsymbol{\nabla}_{\mathbf{k}}\ \mathbf{u}_m^{(\beta)}. \tag{34}$$

The polarization operator can then be separated into interband component proportional to $(1-\delta_{nm})$, and intraband component proportional to δ_{nm}. To tighten the notation let us define the dipole matrix elements as

$$\begin{aligned}\mathbf{r}_{nm} &\equiv \boldsymbol{\xi}_{nm} \qquad n\neq m\\ &\equiv 0 \qquad \text{otherwise.}\end{aligned} \tag{35}$$

The polarization is then[14]

$$\hat{\mathbf{P}} = \hat{\mathbf{P}}_e + \hat{\mathbf{P}}_i, \tag{36}$$

where

$$\hat{\mathbf{P}}_e = \frac{e}{V}\sum_{nm\mathbf{k}}\mathbf{r}_{nm}a_n^\dagger a_m, \tag{37}$$

$$\hat{P}_i^b = \frac{ie}{V}\sum_{n\mathbf{k}}a_n^\dagger a_{n;b}, \tag{38}$$

and $b = x,y,z$. The intraband polarization depends on the covariant derivative of a_n

$$a_{n;b} \equiv \big(\frac{\partial}{\partial k^b} - i\xi_{nn}^b\big)a_n, \tag{39}$$

which transforms as a scalar, $a_{n;b}\to a_{n;b}e^{i\phi_n^\beta}$, under local gauge transformations $\psi_n^{(\beta)}\to\psi_n^{(\beta)}e^{i\phi_n^{(\beta)}}$. This should be contrasted with the transformation of $\partial a_n/\partial k^b$ which acquires a gauge-dependent contribution and hence it cannot represent a physical observable.

From Eq. 36, the susceptibility also naturally separates into intraband and interband contributions as

$$\chi = \chi_i + \chi_e. \tag{40}$$

V. CURRENT OPERATOR

The current density is given by

$$\hat{\mathbf{J}} = \frac{e}{V}\int d\mathbf{r}\ \boldsymbol{\psi}^\dagger\hat{\mathbf{v}}\boldsymbol{\psi}, \tag{41}$$

where $\hat{\mathbf{v}} = [\mathbf{r},\hat{H}_0]/i\hbar = \hat{\mathbf{p}}/m + \mu_B^2\boldsymbol{\sigma}\times\mathbf{e}$ is the electron's velocity. In the presence of light, the momentum changes to $\hat{\mathbf{p}}\to\hat{\mathbf{p}}+e\mathbf{A}$, but after the gauge transformation (24), the current has the same expression. In terms of Bloch operators it becomes

$$\hat{\mathbf{J}} = \frac{e}{V}\sum_{nm\mathbf{k}}\mathbf{v}_{nm}a_n^\dagger a_m, \tag{42}$$

where $\mathbf{v}_{nm}\equiv\langle n\mathbf{k}|\hat{\mathbf{v}}|m\mathbf{k}\rangle$. The current satisfies charge conservation and Maxwell's equation

$$\nabla\cdot\hat{\mathbf{j}} + \frac{\partial\hat{\rho}}{\partial t} = 0 \tag{43}$$

$$\frac{d\hat{\mathbf{P}}}{dt} = \hat{\mathbf{J}}, \tag{44}$$

where $\hat{\rho} = e\boldsymbol{\psi}^\dagger\boldsymbol{\psi}$ is the local charge density, $\hat{\mathbf{j}} = (e/2)\boldsymbol{\psi}^\dagger\hat{\mathbf{v}}\boldsymbol{\psi} + (e/2)(\hat{\mathbf{v}}\boldsymbol{\psi})^\dagger\boldsymbol{\psi}$ is the local charge current, and $\hat{\mathbf{P}}$ is the polarization given by Eq. 36. Local particle conservation follows from the equation of motion (EOM) of $\hat{\rho}$ in the standard way. Maxwell's equation is established as follows. From Eqs. 36 and 28 and $i\hbar d\hat{\mathbf{P}}/dt = [\hat{\mathbf{P}}_i + \hat{\mathbf{P}}_e, \hat{H}]$, we obtain

$$i\frac{d\hat{P}^a}{dt} = \frac{e}{V}\sum_{nm\mathbf{k}}\big(i\omega_{n;a}\delta_{nm} + \omega_{mn}r_{nm}^a\big)a_n^\dagger a_m \tag{45}$$

where $\omega_{nm}\equiv\omega_n-\omega_m$. We define the covariant derivative of the matrix element $O_{nm}\equiv\langle n\mathbf{k}|O|m\mathbf{k}\rangle$ between Bloch states n,m at a single crystal momentum by

$$O_{nm;b} \equiv \left[\frac{\partial}{\partial k^b} - i(\xi_{nn}^b - \xi_{mm}^b)\right]O_{nm}, \tag{46}$$

which can be shown to transform as a tensor under gauge transformations. Since the energy bands are the diagonal matrix elements of the Hamiltonian, their covariant derivative reduces to the standard derivative $\omega_{n;a} = \partial\omega_n/\partial k^a = v_n^a = p_n^a/m + \mu_B^2(\boldsymbol{\sigma}\times\mathbf{e})_{nn}^a$. On the right hand side of Eq. 45, we recognize the diagonal and off-diagonal matrix elements of the velocity. The off-diagonal matrix elements are obtained by taking Bloch matrix elements on both sides of $\hat{\mathbf{v}} = [\mathbf{r}, \hat{H}]/i\hbar$. Comparing with Eq. 42, the Maxwell's equation is established in the basis of Bloch operators.

The intraband polarization operator defines the intraband current operator which, as shown below, connects the semiclassical wavepacket dynamics and the BPVEs.

A. Intraband current

We define the intraband current operator as the time derivative of the intraband polarization operator $\hat{\mathbf{J}}_i = d\hat{\mathbf{P}}_i/dt$. Similarly, the interband current is $\hat{\mathbf{J}}_e = d\hat{\mathbf{P}}_e/dt$. The total current is the sum of the two

$$\hat{\mathbf{J}} = \hat{\mathbf{J}}_i + \hat{\mathbf{J}}_e. \tag{47}$$

Let us first calculate $\hat{\mathbf{J}}_e$ from

$$i\hbar\frac{d\hat{P}_e^a}{dt} = [\hat{P}_e^a, \hat{H}_0] - V\sum_b [\hat{P}_e^a, \hat{P}_i^b + \hat{P}_e^b]E^b. \tag{48}$$

The first term has been computed in Eq. (45). The second term is

$$[\hat{P}_e^a, \hat{P}_i^b + \hat{P}_e^b] = -\frac{ie^2}{V^2}\sum_{nm\mathbf{k}}\left(r_{nm;b}^a + i\sum_p [r_{np}^a r_{pm}^b - r_{np}^b r_{pm}^a]\right)a_n^\dagger a_m. \tag{49}$$

To make progress we now invoke a sum rule first discussed by Sipe and coworkers.[39] It derives from taking matrix elements of

$$[r^a, r^b] = 0, \tag{50}$$

and carefully separating the interband and intraband parts of the position operator shown in Eq. 33. It is easy to show that such procedure works for spinor matrix elements too. Two cases are of interest follow. Taking diagonal matrix elements ($n = m$) of Eq. 50 gives

$$\Omega_n^{ba} \equiv \frac{\partial\xi_{nn}^a}{\partial k^b} - \frac{\partial\xi_{nn}^b}{\partial k^a} = -i\sum_l [r_{nl}^a r_{ln}^b - r_{nl}^b r_{ln}^a], \tag{51}$$

and off-diagonal elements ($m \neq n$) gives

$$r_{nm;b}^a - r_{nm;a}^b = -i\sum_l [r_{nl}^a r_{lm}^b - r_{nl}^b r_{lm}^a]. \tag{52}$$

It is customary, in analogy with electrodynamics, to define a gauge field tensor Ω_n^{ab} derived from the Berry vector potential of band n. The Berry curvature $\boldsymbol{\Omega}_n = \boldsymbol{\nabla}\times\boldsymbol{\xi}_{nn}$ is related to the gauge field by $\Omega_n^{ab} = \sum_e \epsilon_{abe}\Omega_n^e$. We now separate the diagonal from the nondiagonal matrix elements in Eq. 49 and use Eqs. (51,52) to obtain

$$-V\sum_b [\hat{P}_e^a, \hat{P}_i^b + \hat{P}_e^b]E^b = \frac{ie^2}{V}\sum_{n\mathbf{k}}(\mathbf{E}\times\boldsymbol{\Omega}_n)^a a_n^\dagger a_n + \frac{ie^2}{V}\sum_{nm\mathbf{k}b} E^b r_{nm;a}^b\, a_n^\dagger a_m. \tag{53}$$

Subtracting $\hat{\mathbf{J}}_e$ (Eq. 48) from $\hat{\mathbf{J}}$ (Eq. 45) we obtain $\hat{\mathbf{J}}_i$

$$\hat{J}_i^a = \frac{e}{V}\sum_{nm\mathbf{k}}\Big[\omega_{n;a}\delta_{nm} - \frac{e}{\hbar}(\mathbf{E}\times\boldsymbol{\Omega}_n)^a\delta_{nm} - \frac{e}{\hbar}\mathbf{E}\cdot\mathbf{r}_{nm;a}\Big]\, a_n^\dagger a_m. \tag{54}$$

This is an important result. The first term is the standard group velocity (renormalized by the SOC) of an electron wavepacket in band n, $\omega_{n;a} = v_n^a$. As shown below, this term gives rise to the injection current contribution to the BPVE. The second term depends on the Berry curvature $\boldsymbol{\Omega}_n$ and is often called 'anomalous' velocity. It gives rise to many topological effects in condensed matter physics. For example, it gives rise to the (intrinsic) anomalous Hall conductivity in metallic ferromagnets,[1,49] and, as can be easily shown[50], to the (intrinsic) nonlinear Hall effect in nonmagnetic metals.[51,52] In insulators, this term contributes to third order in the electric field but not to second order.

The third term resembles a small dipole created by the external electric field. Just as the standard momentum derivative of Bloch energies leads to the usual group velocity, the (covariant) derivative of the dipole energy $U_{nm} = e\mathbf{E}\cdot\mathbf{r}_{nm}$, can be thought of as a group velocity

$$v_{dip,nm}^a = -\frac{e}{\hbar}\mathbf{E}\cdot\mathbf{r}_{nm;a} \tag{55}$$

associated with a *pair* of wavepackets in distinct bands.

The first two integrands in Eq.(54) are gauge invariant and are usually interpreted as velocity contributions of electron wavepackets.[53] The dipole velocity, on the other hand, is not gauge invariant and hence is not a physical velocity. The dipole current, on the other hand, is gauge invariant and, in this context, the dipole velocity can be given a the interpretation of the velocity of pairs of wavepackets. As shown below, the dipole velocity gives rise to the shift current contribution to the BPVE. In summary, the intraband current unifies the well-known semiclassical dynamics of wavepackets with the BPVEs.

Up to this point, the above formalism is valid for metals and insulators. We now focus on the short time

response of insulators, discarding Fermi surface contributions and momentum relaxation. By 'short time' we mean shorter than momentum relaxation characteristic time (∼100 fs) but longer than the period of light (∼2 fs). The BPVE in this regime has been explored using ultrafast THz spectroscopy in various materials[11,23,24,26–28].

VI. PERTURBATION THEORY

Let us define the single-particle density matrix

$$\rho_{mn} \equiv \langle a_n^\dagger a_m \rangle, \tag{56}$$

where the a_n operators are in the Heisenberg representation and the quantum average is over the ground state defined in the infinite past. The ground state has all the valence bands filled and all conduction bands empty. Being noninteracting, the system is completely characterized by the single-particle density matrix. The amplitude of the electric field is

$$E^b = \sum_\beta E^b_\beta e^{-i(\omega_\beta + i\epsilon)t}, \tag{57}$$

where $\beta = 1, 2, ...$ labels the frequency components of the field. The dipole Hamiltonian is treated as a perturbation with the electric field being turned on slowly in the infinite past so that all the transients effects have vanished. As usual, this is accomplished by taking the limit $\epsilon \to 0$ at the end of the calculation. To find the density matrix we first compute its EOM[14]

$$\frac{\partial \rho_{mn}}{\partial t} + i\omega_{mn}\rho_{mn} = \frac{e}{i\hbar}\sum_{lb} E^b(\rho_{ml}r^b_{ln} - r^b_{ml}\rho_{ln}) - \frac{e}{\hbar}\sum_b E^b \rho_{mn;b}. \tag{58}$$

The first term on the right comes from interband processes as can be recognized by the presence of $\mathbf{r}_{nm}$. The second term comes from the intraband processes which involves the covariant derivative of the density matrix

$$\rho_{mn;b} \equiv \left[\frac{\partial}{\partial k^b} - i(\xi^b_{mm} - \xi^b_{nn})\right]\rho_{mn}, \tag{59}$$

Only when the intraband and interband motion is considered on an equal footing, the EOM reduces to the Boltzmann equation (in the one-band limit) with no collision integral (or the standard semiclassical EOM in a homogeneous electric field).

A. 0th order

If $\mathbf{E} = 0$ the solution of Eq.(58) is simply $\rho^{(0)}_{mn} = \delta_{nm} f_n$, where $f_n \equiv f(\epsilon_n(\mathbf{k})) = 0, 1$ is the Fermi occupation of band n at zero temperature.

B. 1st order

Substituting the 0th order solution into the right-hand side of Eq.(58) and solving for $\rho^{(1)}_{mn}$ we obtain

$$\rho^{(1)}_{mn} \equiv \sum_{b\beta} \bar{\rho}^{(1)b\beta}_{mn} E^b_\beta e^{-i\omega_\beta t} \tag{60}$$

$$= \frac{e}{\hbar}\sum_{b\beta} \frac{r^b_{mn} f_{nm}}{\omega_{mn} - \omega_\beta} E^b_\beta e^{-i\omega_\beta t}. \tag{61}$$

where we defined $f_{nm} \equiv f_n - f_m$. Note that to first order only the interband processes are allowed in insulators.

C. 2nd order

To second order we have

$$\rho^{(2)}_{mn} \equiv \sum_{b\beta}\sum_{c\sigma} \bar{\rho}^{(2)b\beta c\sigma}_{mn} E^b_\beta E^c_\sigma e^{-i\omega_\Sigma t}, \tag{62}$$

where

$$\bar{\rho}^{(2)b\beta c\sigma}_{mn} = \frac{ie}{\hbar(\omega_{mn} - \omega_\Sigma)}\Big[\bar{\rho}^{(1)b\beta}_{mn;c} + i\sum_l \left(\bar{\rho}^{(1)b\beta}_{ml} r^c_{nl} - r^c_{ml}\bar{\rho}^{(1)b\beta}_{ln}\right)\Big], \tag{63}$$

and $\omega_\Sigma = \omega_\beta + \omega_\sigma$. The covariante derivative of a quotient in $\bar{\rho}^{(1)b\beta}_{mn;c}$ is simply

$$\left(\frac{r^a_{mn} f_{nm}}{\omega_{mn} - \omega_\alpha}\right)_{;b} = \frac{r^a_{mn;b} f_{nm}}{\omega_{mn} - \omega_\alpha} - \frac{r^a_{mn} f_{nm} \omega_{mn;b}}{(\omega_{mn} - \omega_\alpha)^2} \tag{64}$$

D. nth-order

In the long-time limit, by which we mean longer than the period of light, we expect harmonic solutions of the form

$$\rho^{(n)}_{mn} = \sum_{a_1\alpha_1,...} \bar{\rho}^{(n)a_1\alpha_1,...}_{mn} E^{a_1}_{\alpha_1} \cdots E^{a_n}_{\alpha_n} e^{-i\omega^{(n)}_\Sigma t}, \tag{65}$$

where $\omega^{(n)}_\Sigma = \omega_{\alpha_1} + \cdots + \omega_{\alpha_n}$. Substituting into Eq.(58) and iterating we obtain an equation for $\bar{\rho}^{(n+1)}_{mn}$ in terms of $\bar{\rho}^{(n)}_{mn}$. Omitting the supercripts $a_1\alpha_1, ...$ for clarity we obtain

$$\bar{\rho}^{(n+1)}_{mn} = \frac{ie}{\hbar(\omega_{mn} - \omega^{(n+1)}_\Sigma)}\Big[i\sum_l (\bar{\rho}^{(n)}_{ml} r^{a_{n+1}}_{ln} - r^{a_{n+1}}_{ml}\bar{\rho}^{(n)}_{ln}) + \bar{\rho}^{(n)}_{mn;a_{n+1}}\Big]. \tag{66}$$

Note that at every order in perturbation theory there are interband (first term) and intraband (second term) contributions. In general, the nth-order $\rho^{(n)}$ ($n \geq 1$) has 2^{n-1} intraband and 2^{n-1} interband contributions.

VII. PHYSICAL DIVERGENCES OF χ_2

In the long-time limit, the susceptibility and conductivity response tensors to second order are defined by

$$P^{a(2)} \equiv \sum_{b\beta c\sigma} \chi_2^{abc}(-\omega_\Sigma, \omega_\beta, \omega_\sigma) E^b_\beta E^c_\beta e^{-i\omega_\Sigma t}, \tag{67}$$

$$J^{a(2)} \equiv \sum_{b\beta c\sigma} \varsigma_2^{abc}(-\omega_\Sigma, \omega_\beta, \omega_\sigma) E^b_\beta E^c_\beta e^{-i\omega_\Sigma t}, \tag{68}$$

where $\omega_\Sigma = \omega_\beta + \omega_\sigma$. They are related by $dP^{a(2)}/dt = J^{a(2)}$. χ_2 can be split into interband and intraband components $\chi_2 = \chi_{2e} + \chi_{2i}$ using Eqs.(37),(54),(61), and (63). The result is[39]

$$\frac{\chi^{abc}_{2e}}{C_2} = i \sum_{nm\mathbf{k}} \frac{r^a_{nm} f_{nm}}{\omega_{mn} - \omega_\Sigma} \left(\frac{r^b_{mn}}{\omega_{mn} - \omega_\beta} \right)_{;c} - \sum_{nlm\mathbf{k}} \frac{r^a_{nm}}{\omega_{mn} - \omega_\Sigma} \left(\frac{r^b_{ml} r^c_{ln} f_{lm}}{\omega_{ml} - \omega_\beta} - \frac{r^c_{ml} r^b_{ln} f_{nl}}{\omega_{ln} - \omega_\beta} \right), \tag{69}$$

$$\frac{\chi^{abc}_{2i}}{C_2} = \frac{i}{\omega^2_\Sigma} \sum_{nm\mathbf{k}} \frac{\omega_{nm;a} r^b_{nm} r^c_{mn} f_{mn}}{\omega_{nm} - \omega_\beta} + \frac{1}{i\omega_\Sigma} \sum_{nm\mathbf{k}} \frac{r^c_{nm;a} r^b_{mn} f_{nm}}{\omega_{mn} - \omega_\beta}, \tag{70}$$

where we defined $C_2 = e^3/\hbar^2 V$. These expressions need to be symmetrized with respect to exchange of indices $b\beta \leftrightarrow c\sigma$. We note that χ_{2i} is easier to calculate from $\mathbf{J}^{(2)}_i$ rather than directly from $\mathbf{P}^{(2)}_i$.

The Taylor expansion of χ_{2i} in Eq. 4[14,39] means that χ_{2i} diverges as $\omega_\Sigma \to 0$ and that the injection η_2 and shift σ_2 response tensors can be obtained from this expansion, see Appendix B. Here we derive these tensors from a slightly different perspective that exposes the analytic properties of χ_{2i}. Let us assume χ_{2i} admits a Laurent series

$$\chi_{2i} = \frac{\eta_2}{z^2} + \frac{\sigma_2}{z} + \cdots \tag{71}$$

where $z = -i\omega_\Sigma$. Then η_2 is given by

$$\eta_2 = \frac{1}{2\pi i} \oint_{|z|=\rho} dz\ z \chi_{2i}, \tag{72}$$

where ρ is the radius of convergence. All the frequencies are parametrized in terms of $\omega_\Sigma = iz$. One such parametrization is

$$\omega_\beta = \omega + n_\beta \omega_\Sigma \tag{73}$$

$$\omega_\sigma = -\omega + n_\sigma \omega_\Sigma, \tag{74}$$

where $n_\beta + n_\sigma = 1$. The manifold where $\omega_\Sigma = 0$ is a line of singular points $(\omega_\beta, \omega_\sigma) = (\omega, -\omega)$, parametrized by a single frequency $\omega > 0$. Symmetrizing χ_{2i} with respect to exchange of indices $b\beta \leftrightarrow c\sigma$ and using Eq. 72 we obtain $\eta_2^{abc}(0, \omega, -\omega)$ as

$$\eta_2^{abc} = \frac{\pi e^3}{\hbar^2 V} \sum_{nm\mathbf{k}} f_{mn}\ \omega_{nm;a} r^b_{nm} r^c_{mn} \delta(\omega_{nm} - \omega), \tag{75}$$

or equivalently

$$\eta_2^{abc} = \frac{\pi e^3}{2\hbar^2 V} \sum_{nm\mathbf{k}} f_{mn} \omega_{nm;a} (r^b_{nm} r^c_{mn} - r^c_{nm} r^b_{mn}) \times \delta(\omega_{nm} - \omega), \tag{76}$$

which are both independent of the parameters n_β, n_σ. In calculating η_2 we take the limit $\rho \to 0$ before the limit $\epsilon \to 0$. This corresponds to the physical situation where $\omega_\Sigma = 0$ in the infinite past. Similarly, $\sigma_2^{abc}(0, \omega, -\omega)$ is given by

$$\sigma_2 = \frac{1}{2\pi i} \oint_{|z|=\rho} dz\ \chi_{2i}. \tag{77}$$

An explicit integration gives

$$\sigma_2^{abc} = \frac{i\pi e^3}{2\hbar^2 V} \sum_{nm\mathbf{k}} f_{mn} (r^c_{nm;a} r^b_{mn} - r^c_{nm} r^b_{mn;a}) \delta(\omega_{nm} - \omega). \tag{78}$$

In calculating σ_2 we took $n_\beta = n_\sigma = 1/2$ to eliminate a resonant imaginary term which depends on $n_\beta - n_\sigma$. This term does not arise in the standard method[14,39] because there the prescription is to Taylor expand only the real parts. Taking $n_\beta = n_\sigma$ means we are approaching the line of singularities at right angle.

Eqs.(75) and (78) are the well-known injection and shift current tensors. η_2 is pure imaginary and antisymmetric in b, c indices and hence vanishes for linear polarization[5]. σ_2, on the other hand, is real, symmetric in b, c indices and hence vanishes for circular polarization. Following the standard convention,[38] the injection and shift currents are

$$J^{a(2)}_{sh} \equiv \sum_{b\beta c\sigma} \sigma_2^{abc}(-\omega_\Sigma, \omega_\beta, \omega_\sigma) E^b_\beta E^c_\sigma e^{-i\omega_\Sigma t}$$

$$\frac{d}{dt} J^{a(2)}_{inj} \equiv \sum_{b\beta c\sigma} \eta_2^{abc}(-\omega_\Sigma, \omega_\beta, \omega_\sigma) E^b_\beta E^c_\sigma e^{-i\omega_\Sigma t}. \tag{79}$$

Assuming a monocromatic source $E(\omega)e^{-i\omega t} + c.c.$ and performing the frequency sums keeping only dc terms ($\omega_\Sigma = 0$), we obtain

$$J^{a(2)}_{sh} = 2 \sum_{bc} \sigma_2^{abc}(0, \omega, -\omega) E^b(\omega) E^c(-\omega) \tag{80}$$

$$\frac{d}{dt} J^{a(2)}_{inj} = 2 \sum_{bc} \eta_2^{abc}(0, \omega, -\omega) E^b(\omega) E^c(-\omega), \tag{81}$$

where the factor of 2 is from the intrinsic permutation symmetry of susceptibilities.[38] Being quadratic in the

fields they vanish for centrosymmetric systems. The above expressions indicate the injection and shift currents vary as

$$|\mathbf{J}^{(2)}_{inj}(t)| \sim \eta_2 t \tag{82}$$

$$|\mathbf{J}^{(2)}_{sh}(t)| \sim \sigma_2 \tag{83}$$

with illumination time in the absence of momentum relaxation and saturation effects.

A. Physical interpretation of injection and shift current

In this section we show that the injection and shift currents can be understood from simple semiclassical wavepacket dynamics.

1. *Injection current*

The physical origin of the injection current is well known. It arises from the asymmetry in the carrier injection rate at time-reversed momenta in the BZ[5,32]. To see this, let us consider an electron wavepacket with velocity v^a_n. The current is

$$J^a = \frac{e}{V}\sum_{n\mathbf{k}} f_n v^a_n, \tag{84}$$

where $f_n \equiv \rho^{(0)}_{nn}$. The effect of an optical field is to *inject* carriers into the current-carrying states in the conduction bands. Taking a time derivative of the occupation we obtain

$$\frac{d}{dt}J^a_{inj} = \frac{e}{V}\sum_{n\mathbf{k}} \frac{df_n}{dt} v^a_n. \tag{85}$$

For low intensity, the Fermi's Golden Rule gives the one-photon absorption rate[32]

$$\frac{df_v}{dt} = -\frac{2\pi e^2}{\hbar^2}\sum_c |\mathbf{E}(\omega)\cdot\mathbf{r}_{cv}|^2\delta(\omega_{cv}-\omega)$$

$$\frac{df_c}{dt} = \frac{2\pi e^2}{\hbar^2}\sum_v |\mathbf{E}(\omega)\cdot\mathbf{r}_{cv}|^2\delta(\omega_{cv}-\omega), \tag{86}$$

where c, v labels a conduction or a valence band respectively. For complex fields, e.g, circularly polarized or elliptically polarized light, the carrier injection rate at time-reversed points $\pm\mathbf{k}$ in the BZ is not the same

$$\frac{d}{dt}f_c(-\mathbf{k}) \neq \frac{d}{dt}f_c(\mathbf{k}), \tag{87}$$

leading to a polar distribution of Bloch velocity states. This is the microscopic origin of the injection current and, as we show below, of many higher order injection currents. Substituting into Eq.(85) we obtain the injection current as

$$\frac{d}{dt}J^{a(2)}_{inj} = \frac{2\pi e^3}{\hbar^2 V}\sum_{b'c'}\sum_{cv\mathbf{k}} \omega_{cv;a} r^{b'}_{vc} r^{c'}_{cv}\delta(\omega_{cv}-\omega)$$
$$\times E^{b'}(\omega)E^{c'}(-\omega), \tag{88}$$

or

$$\frac{d}{dt}J^{a(2)}_{inj} = \frac{2\pi e^3}{\hbar^2 V}\sum_{bc}\sum_{nm\mathbf{k}} f_{mn}\omega_{nm;a} r^{b}_{nm} r^{c}_{mn}\delta(\omega_{nm}-\omega)$$
$$\times E^{b}(\omega)E^{c}(-\omega), \tag{89}$$

which is the standard injection current shown in Eq.(81).

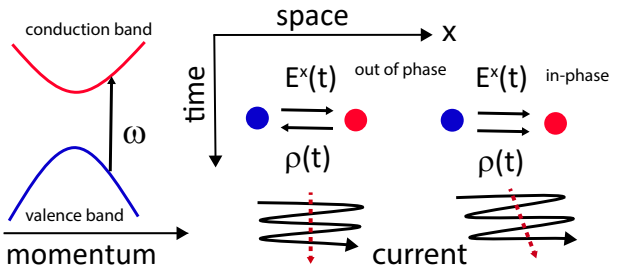

FIG. 1. Intuitive picture of microscopic generation of shift current. The wiggle lines represent particle-hole oscillations between the valence and conduction band centers of charge (circles) which are spatially separated. The quantum interference between population oscillations $\rho_{nm}(t)$ and dipole oscillations $\mathbf{E}(t)\cdot\mathbf{r}_{mn}$ gives rise to a dc current.

2. *Shift current*

Injection current is proportional to the momentum relaxation time and hence explicitly breaks time-reversal symmetry. The shift current, on the other hand, does not require the presence of momentum relaxation[8] to break time reversal symmetry. In this sense, shift current is like the dissipationless Hall conductivity.[54] In the quantum Hall effect, time reversal symmetry is broken by a magnetic field. How is time-reversal symmetry broken in the shift current? It is broken at the time of photon absorption which is an irreversible process.

Materials that exhibit shift current have valence and conduction band centers spatially separated within the unit cell and hence charge is *shifted* upon photon absorption. This process depends only on the off-diagonal density matrix elements and hence it requires quantum coherence as has been extensively documented. Here we propose that shift current arises from the quantum interference of two distinct microscopic processes involving wavepacket oscillations in the presence of an electric field.

To see this consider the dipole current in Eq.(54) to second order

$$J^{a(2)}_{dip} = -\frac{e^2}{\hbar V}\sum_{nm\mathbf{k}} \mathbf{E}(t)\cdot \mathbf{r}_{nm;a}\ \rho^{(1)}_{mn}(t). \tag{90}$$

The total current is the sum of dipole velocities for each pair of wavepackets in bands n, m weighted by the probability $\rho^{(1)}_{mn}$ of being occupied. From Eq. 61 we have

$$J^{a(2)}_{dip} = -\frac{e^3}{\hbar^2 V}\sum_{b\beta c\sigma}\sum_{nm\mathbf{k}} \frac{r^b_{nm;a} r^c_{mn} f_{nm}}{\omega_{mn}-\omega_\sigma} E^b_\beta E^c_\sigma e^{-i\omega_\Sigma t}, \tag{91}$$

where $\omega_\Sigma = \omega_\beta + \omega_\sigma$. Symmetrizing with respect to exchange of indices $b\beta \leftrightarrow c\sigma$, assuming a monocromatic field $E^b = E^b(\omega)e^{-i\omega t} + c.c.$, and keeping only the dc resonant terms we obtain

$$J^{a(2)}_{sh} = \frac{i\pi e^3}{\hbar^2 V}\sum_{bc}\sum_{nm\mathbf{k}} f_{mn}(r^b_{nm;a} r^c_{mn} + r^c_{nm;a} r^b_{mn}) \times\delta(\omega_{nm}-\omega) E^b(\omega) E^c(-\omega), \tag{92}$$

Which is the standard expression for the shift current in Eq. 80. This calculation suggests that the *quantum* mechanical interference of population and dipole oscillations is the microscopic origin of the shift current, see Fig. 1. We note that electron oscillations between centers of charge, alone, do not lead to a dc current. However, the directionality of the electron oscillations combined with an isotropic relaxation (due to, e.g., randomized collisions) could, in principle, also lead to a dc current.

We now show how the injection and shift currents are modified by the presence of a static electric field.

VIII. PHYSICAL DIVERGENCES OF χ_3

In the long-time limit, the susceptibility and conductivity response tensors to third order are defined by

$$P^{a(3)} = \sum_{b\beta c\sigma d\delta} \chi_3^{abcd}(-\omega_\Sigma,\omega_\beta,\omega_\sigma,\omega_\delta) E^b_\beta E^c_\sigma E^d_\delta e^{-i\omega_\Sigma t}, \tag{93}$$

$$J^{a(3)} = \sum_{b\beta c\sigma d\delta} \sigma^{abcd(3)}(-\omega_\Sigma,\omega_\beta,\omega_\sigma,\omega_\delta) E^b_\beta E^c_\sigma E^d_\delta e^{-i\omega_\Sigma t}, \tag{94}$$

where $\omega_\Sigma = \omega_\beta+\omega_\sigma+\omega_\delta$. They are related by $d\mathbf{P}^{(3)}/dt = \mathbf{J}^{(3)}$. χ_3 can be split into interband and intraband components $\chi_3 = \chi_{3e} + \chi_{3i}$. An explicit calculation gives

$$(-i\omega_\Sigma)^3\chi_{3i} = \iota_3 + (-i\omega_\Sigma)\eta_3 + (-i\omega_\Sigma)^2\sigma_3 + \cdots. \tag{95}$$

See Appendix D. The same expression was obtained in Ref. 39. The difference is that we calculate the intraband current J^a_i explicitly and use it to guide our physical intuition about the singularities of χ_{3i}. Eq.(95) is equivalent to

$$\chi_{3i} = \frac{\iota_3}{z^3} + \frac{\eta_3}{z^2} + \frac{\sigma_3}{z} + \cdots \tag{96}$$

where $z \equiv -i\omega_\Sigma$. Since χ_{3e} is regular, Eq. 96 implies that the conductivity in the limit of no momentum relaxation is

$$\sigma^{(3)} = \frac{\iota_3}{z^2} + \frac{\eta_3}{z} + \sigma_3 + z(reg), \tag{97}$$

where reg represents the remaining regular terms (as $z\to 0$). The residues ι_3, η_3 and σ_3 define various current contributions as follows. The limit

$$\lim_{z\to 0} z^2\sigma^{(3)} = \iota_3, \tag{98}$$

or equivalently

$$\lim_{\omega_\Sigma\to 0}\frac{d^2}{dt^2}J^{a(3)} \equiv \frac{d^2}{dt^2}J^{a(3)}_{jerk} = \sum_{b\beta c\sigma d\delta}\iota_3^{abcd}(0,\omega_\beta,\omega_\sigma,\omega_\delta)E^b_\beta E^c_\beta E^d_\delta, \tag{99}$$

subject to $\omega_\Sigma = 0$ defines the jerk current. Similarly the limits

$$\lim_{z\to 0} z\left[\sigma^{(3)} - \frac{\iota_3}{z^2}\right] = \eta_3, \tag{100}$$

$$\lim_{z\to 0}\left[\sigma^{(3)} - \frac{\iota_3}{z^2} - \frac{\eta_3}{z}\right] = \sigma_3, \tag{101}$$

define higher order injection and shift currents (respectively) in the presence of a static electric field:

$$\frac{d}{dt}J^{a(3)}_{inj} \equiv \sum_{b\beta c\sigma d\delta}\eta_3^{abcd}(0,\omega_\beta,\omega_\sigma,\omega_\delta)E^b_\beta E^c_\beta E^d_\delta, \tag{102}$$

$$J^{a(3)}_{sh} \equiv \sum_{b\beta c\sigma d\delta}\sigma_3^{abcd}(0,\omega_\beta,\omega_\sigma,\omega_\delta)E^b_\beta E^c_\beta E^d_\delta, \tag{103}$$

subject to $\omega_\Sigma = 0$. We now analyze each of these currents in detail.

IX. JERK CURRENT

A. Hydrodynamic model

In an isotropic system the current is

$$J^a_{clas} = env^a, \tag{104}$$

where n is the carrier density. Taking two derivatives we obtain

$$\frac{d^2}{dt^2}J^a_{clas} = e\frac{d^2n}{dt^2}v^a + 2e\frac{dn}{dt}\frac{dv^a}{dt} + en\frac{d^2v^a}{dt^2}. \quad (105)$$

If the rate of carrier injection $dn/dt = g$ and acceleration eE^a_0/m^* are constant in time then

$$\frac{d^2}{dt^2}J^a_{clas} = \frac{2e^2gE^a_0}{m^*} = constant, \quad (106)$$

leads to a current varying quadratically with illumination time. This effect has been extensively studied in the context of the THz generation in bias semiconductor antennas using semiclassical kinetic equations, see for example Ref. 46. However, the static field modifies the carrier injection rate giving rise to novel contributions. The sum of all contributions is called the jerk current. We now discuss this effect.

B. Susceptibility divergence

We find ι_3 from the limit $\lim_{\omega_\Sigma\to 0}(-i\omega_\Sigma)^3\chi_{3i} = \iota_3$. The details of the derivation are outlined in Appendix D. $\iota_3^{abcd}(0,\omega,-\omega,0)$ is given by[40]

$$\iota_3^{abcd} = \frac{2\pi e^4}{6\hbar^3 V}\sum_{nm\mathbf{k}} f_{mn}\big[2\omega_{nm;ad}r^b_{nm}r^c_{mn} + \omega_{nm;a}(r^b_{nm}r^c_{mn})_{;d}\big]\delta(\omega_{nm}-\omega), \quad (107)$$

where $\omega_{nm;ad} = \partial^2\omega_{nm}/\partial k^d\partial k^a = \partial^2\omega_n/\partial k^d\partial k^a - \partial^2\omega_m/\partial k^d\partial k^a$.

Assuming time-reversal symmetry in the ground state we can choose $\mathbf{r}_{nm}(-\mathbf{k}) = \mathbf{r}_{mn}(\mathbf{k})$ to show that ι_3 is real, symmetric in the b,c indices, and satisfies $[\iota_3^{abcd}(0,\omega,-\omega,0)]^* = \iota_3^{acbd}(0,\omega,-\omega,0) = \iota_3^{abcd}(0,-\omega,\omega,0)$. From Eq. 99, we see that ι_3 controls the current

$$\frac{d^2}{dt^2}J^{a(3)}_{jerk} = \sum_{b\beta c\gamma d\delta}\iota_3^{abcd}(-\omega_\Sigma,\omega_\beta,\omega_\gamma,\omega_\delta)E^b_\beta E^c_\gamma E^d_\delta e^{-i\omega_\Sigma t}, \quad (108)$$

subject to $\omega_\Sigma = 0$. Performing the sum over frequencies we obtain

$$\frac{d^2}{dt^2}J^{a(3)}_{jerk} = 6\sum_{bcd}\iota_3^{abcd}(0,\omega,-\omega,0)E^b(\omega)E^c(-\omega)E^d_0, \quad (109)$$

where E^d_0 is a static external field. The factor of $6 = 3!$ is the number of pair-wise exchanges of field indices $(b\beta),(c\sigma),(d\delta)$.[38] The jerk current vanishes for frequencies smaller than the energy band gap. Eq.(109) indicates that the jerk current grows quadratically with illumination time

$$|\mathbf{J}^{(3)}_{jerk}(t)| \sim \iota_3 t^2, \quad (110)$$

in the absence of momentum relaxation and saturation effects. In analogy with second derivative of velocity which is called 'jerk' we dub it *jerk* current. This should be compared and contrasted with injection current which grows linearly with illumination time (Eq. 82) and shift current which is constant (Eq. 83).

Two terms contribute to the jerk current. The first depends on the curvature difference of the bands involved, or equivalently on inverse mass differences. This term is related to the stiffness of the lattice and can also be interpreted as the electron acceleration in the static electric field. The second contribution depends on the change of transition probabilities due to the static field.

C. Materials

In general, the 81 components of ι_3 are finite in both centrosymmetric and noncentrosymmetry crystal structures. In practice, the symmetries of the 32 crystal classes greatly reduce the number of independent components. For example, GaAs has $\bar{4}3m$ point group, with 21 nonzero components and 4 independent components.[38] However, ι_3 is symmetric under exchange of bc which reduces the number of independent component to 3. In 2D materials the number of components of ι_3 is also small. For example, single-layer GeS has $mm2$ point group which contains a mirror-plane symmetry and a 2-fold axis. In this case ι_3 has only six independent components.

In general, linear, circular or unpolarized light will produce jerk current along the direction of the static field. Current transverse to the static field may not be generated with unpolarized or circular polarization.

D. Physical interpretation of jerk current

The terms in Eq.(107) are hard to interpret physically. We now rederive the same result in a physically more transparent way using a phenomenological model.[40] Consider an electron wavepacket in band n subject to a static electric field E^d_0. The electron's wavevector obeys

$$\hbar\frac{d\mathbf{k}}{dt} = -e\frac{\partial\mathbf{A}_0}{\partial t}, \quad (111)$$

where the vector potential $\mathbf{A}_0$ gives the static electric field $E^d_0 = -\partial A^d_0/\partial t$. The Bloch velocity of the electron $\mathbf{v}_n(\mathbf{k} - e\mathbf{A}_0/\hbar)$ can be expanded in powers of $\mathbf{A}_0$. The time derivatives of this expression have a simple form as powers of the field. For example, the 1st and 2nd derivatives are given by

$$\frac{dv^a_n}{dt} = \frac{e}{\hbar}\sum_d \omega_{n;ad}E^d_0 \quad (112)$$

$$\frac{d^2v^a_n}{dt^2} = \frac{e^2}{\hbar^2}\sum_{de}\omega_{n;ade}E^d_0E^e_0. \quad (113)$$

Now, taking two time derivatives of Eq.(84)

$$\frac{d^2J^a}{dt^2} = \frac{e}{V}\sum_{n\mathbf{k}}\left(\frac{d^2f_n}{dt^2}v_n^a + 2\frac{df_n}{dt}\frac{dv_n^a}{dt} + f_n\frac{d^2v_n^a}{dt^2}\right). \tag{114}$$

and using Eq.(112), and (86) we have (to linear order in E_0^d)

$$\begin{aligned}\frac{d^2}{dt^2}J^{a(3)}_{jerk} &= \\ &\frac{2\pi e^4}{\hbar^3 V}\sum_{bc'd}\sum_{cv\mathbf{k}} 2\omega_{cv;ad}r^b_{vc}r^{c'}_{cv}\delta(\omega_{cv}-\omega)E^b(\omega)E^{c'}(-\omega)E_0^d \\ &+ \frac{2\pi e^4}{\hbar^3 V}\sum_{bc'd}\sum_{cv\mathbf{k}}\omega_{cv;a}\frac{\partial(r^b_{vc}r^{c'}_{cv})}{\partial k^d}\delta(\omega_{cv}-\omega) \\ &\times E^b(\omega)E^{c'}(-\omega)E_0^d. \end{aligned} \tag{115}$$

Since $\omega > 0$ we can extend the sums over to all bands and recover Eq.(109). An important point of this calculation is to show that the physical origin of the first term in Eq.(107) comes from the acceleration of carriers in the static electric field. The second contribution comes from changes in the carrier injection rate, d^2f_n/dt^2 which is missing in the standard semiclassical approach.[46]

E. Jerk Hall current

In an isotropic medium, charge carriers move parallel to the electric field. The jerk current, on the other hand, can flow transverse to the static electric field in a rotationally symmetric medium. To see this, let us assume a sample biased in the x-direction and compute the current in the y-direction while an optical field $\mathbf{E} = \hat{\mathbf{x}}E^x(\omega)e^{-i\omega t} + \hat{\mathbf{y}}E^y(\omega)e^{-i\omega t} + c.c.$, with $E^a(\omega) = |E^a(\omega)|e^{-i\phi_a}$, is incident perpendicular to the sample surface which defines the xy-plane. The current in the $y-$direction is

$$\frac{d^2}{dt^2}J^{y(3)}_{jerk} = \varsigma^{yx}_{3jH}E^x_0, \tag{116}$$

where the effective jerk Hall (jH) conductivity is

$$\begin{aligned}\varsigma^{yx}_{3jH} \equiv\ & 6\iota_3^{yxxx}|E^x(\omega)|^2 + 6\iota_3^{yyyx}|E^y(\omega)|^2 \\ &+ 12\iota_3^{yyxx}|E^x(\omega)||E^y(\omega)|\cos(\phi_x-\phi_y).\end{aligned} \tag{117}$$

In a simple relaxation time approximation jerk conductivity (see Eq. 97) is cut off by a relaxation time τ_1 as

$$\frac{\iota_3}{(-i\omega_\Sigma)^2} \to \frac{\iota_3}{(\frac{1}{\tau_1}-i\omega_\Sigma)^2} \tag{118}$$

Hence, the jerk current is

$$J^{y(3)}_{jerk} = \frac{\tau_1^2}{(1-i\omega_\Sigma\tau_1)^2}\varsigma^{yx}_{3jH}E^x_0, \tag{119}$$

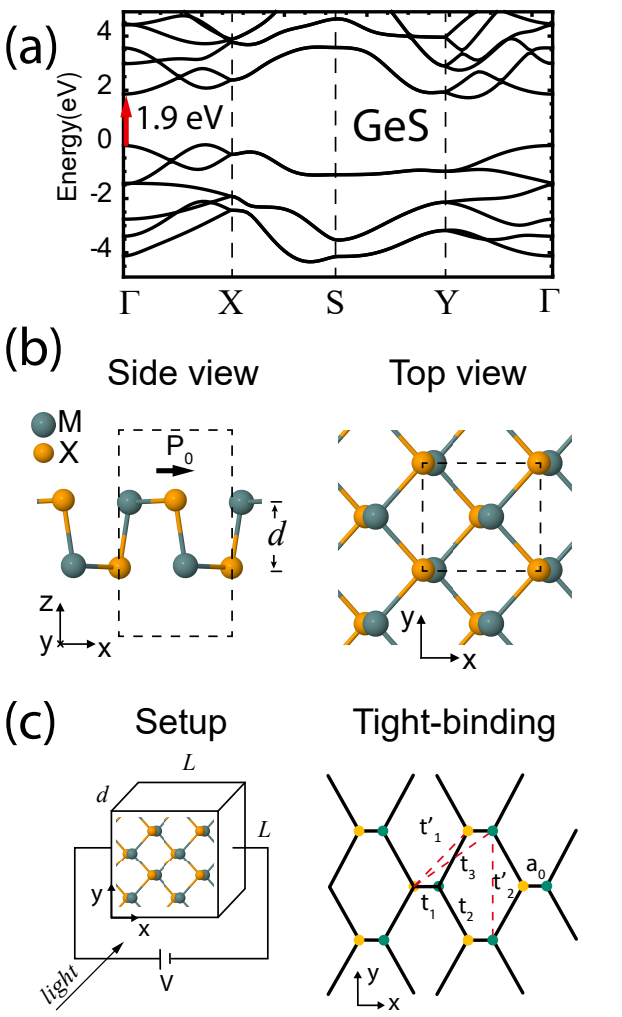

FIG. 2. (a) Band structure of single-layer GeS[13,55] indicating transitions near the band edge (red arrow). (b) crystal structure of single-layer GeS, (c) two-dimensional, two-band tight binding model of single-layer GeS which reproduces the nonlinear optical response of near the band edge. The hopping parameters considered are indicated. See main text for more details.

where τ_1 is the relaxation time of the diagonal density matrix elements. In the dc limit the current is proportional to the square of the momentum relaxation. For frequencies larger than the Drude peak but smaller than interband transitions the current is independent of the scattering time and it is a measure of the geometry of the Bloch wavefunctions.

The dependence on light's polarization as $\cos(\phi_x-\phi_y)$ and the square of the momentum relaxation are unique characteristics of the jerk current which can be used to distinguish it from η_3 and σ_3.

The symmetries of the crystal can also constrain the contributions to the jerk current, e.g., if the crystal has mirror symmetry $y \to -y$ the first and second terms in Eq. 117 vanish. In addition, for circular polarization

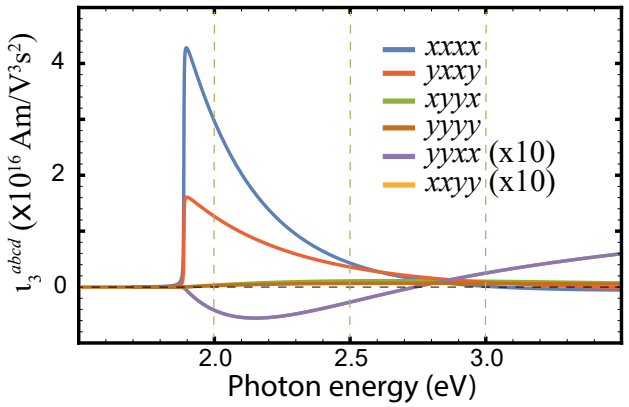

FIG. 3. Jerk current response tensor from the two band model of single-layer GeS. The two-band model is shown in Fig. 2. The tensor vanishes for photon energies lower than the energy band gap (~ 1.9 eV[13,56]). The strongest component is along the polar axis $xxxx$. The components $yyxx, xxyy$, describe a Hall-like response and are an order of magnitude smaller. For added clarity, these components are multiplied by 10 in the figure.

$\phi_x - \phi_y = \pm\pi/2$ the last term vanishes. An estimate of the jerk current in realistic materials is given next.

F. Example: Jerk current in single-layer GeS

To get a sense of the magnitude of the jerk current in real materials we now calculate it for single-layer GeS. Single-layer GeS is of great interest for its predicted in-plane spontaneous ferroelectric polarization, suitable energy band gap in the visible spectrum (~ 1.9 eV) and large nonlinear optical response[11,13,57,58].

We consider a 2D, two-band tight-binding model of single-layer GeS shown in Fig. 2c. The details of the model are presented in Appendix G. The model has been shown to reproduce the *ab-initio* shift and injection current of single-layer GeS near the band edge,[13,56,59] specifically in the energy range 1.9-2.14 eV. Since the model is 2D, we divide the model's 2D current by the thickness of the GeS layer ($d \sim 2.56$Å) to obtain an effective bulk value.

Because of the mirror symmetry $y \to -y$ of the model (and of the crystal), only six tensor component are independent. As seen in Fig. 3, the strongest is along the polar (chosen along x-axis) of magnitude $\sim 10^{16}$ Am/V^{3}s^2. The current transverse to the static electric field, described by the component ι_3^{yyxx} (see Eq. 116), is an order of magnitude smaller.

The sample is rectangular of dimensions $L \times L$ and thickness $d = 2.56$ Å and is biased by an external battery of voltage V, as seen Fig. 2c. Let us assume the optical field is incident perpendicularly to the plane of single-layer GeS as

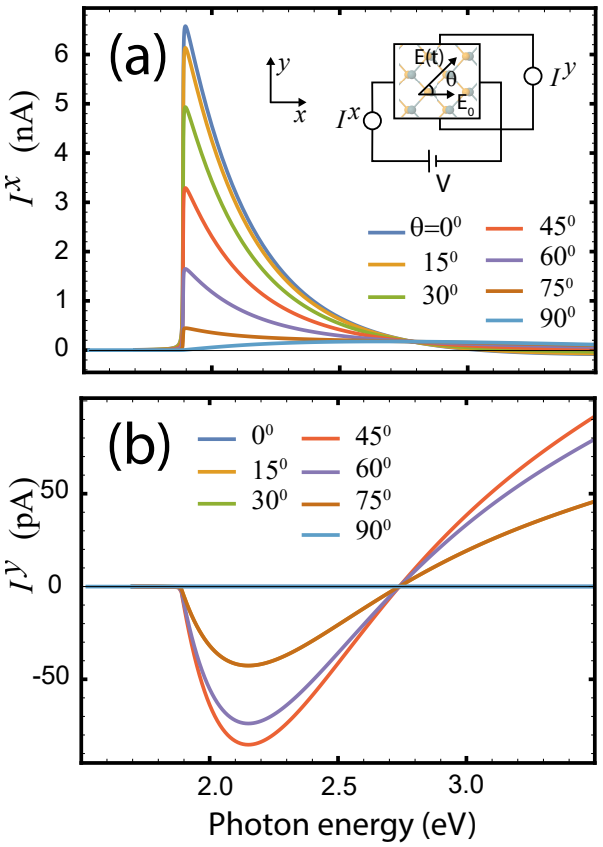

FIG. 4. Total jerk current induced by an optical field incident perpendicular to the plane of single-layer GeS. The inset shows the top view of the setup.

$$\mathbf{E}(t) = \hat{\mathbf{x}}E^x(\omega)e^{-i\omega t} + \hat{\mathbf{y}}E^y(\omega)e^{-i\omega t} + c.c. \quad (120)$$

$$\mathbf{E}_0 = \hat{\mathbf{x}}E_0^x. \quad (121)$$

where $E^x(\omega) = E^0(\omega)\cos\theta e^{-i\phi_x}$, $E^y(\omega) = E^0(\omega)\sin\theta e^{-i\phi_y}$, θ is the angle with the x-axis. The longitudinal and transverse currents are

$$I_{jerk}^{x(3)} = 6A\tau_1^2(\iota_3^{xxxx}|E^x(\omega)|^2 + \iota_3^{xyyx}|E^y(\omega)|^2)E_0^x, \quad (123)$$

$$I_{jerk}^{y(3)} = 12A\tau_1^2\iota_3^{yyxx}|E^x(\omega)||E^y(\omega)|\cos(\phi_x - \phi_y)E_0^x, \quad (124)$$

where $A = Ld$ is the transverse area of the sample. Note that the current along the polar (x)-axis is independent of the polarization of light. Hence, the polar component of the current will not vanish even for unpolarized light. The transverse component of the current, on the other hand, vanishes for circularly polarized (and unpolarized) light and is maximum for linearly polarized light.

The optical field is linearly polarized ($\phi_x = \phi_y$) at an angle θ with the polar axis as shown in the inset to Fig. 4a. The figure shows the total current induced as a function of θ. We assumed semiconductor parameters

$$\eta_3^{abcd}(0,\omega,-\omega,0) = -\frac{\pi e^4}{6\hbar^3 V}\sum_{nm\mathbf{k}} f_{mn}\Big(\Omega^{ad}_{nm}[r^b_{nm},r^c_{mn}] + i[r^b_{nm},r^c_{mn;a}]_{;d} - 2i\omega_{nm;a}\Big[\left(\frac{r^d_{mn}}{\omega_{nm}}\right)_{;b},r^c_{nm}\Big]\Big)\delta(\omega_{nm}-\omega)$$
$$-\frac{\pi e^4}{3\hbar^3 V}\sum_{nml\mathbf{k}} f_{mn}\omega_{nm;a}\frac{r^d_{ln}}{\omega_{nl}}[r^b_{nm},r^c_{ml}]D_-(\omega_{nm},\omega). \tag{122}$$

typically found in the laboratory: $L = 100\mu$m, $V = 1$V, $E^x_0 = V/L = 10^4$ V/m, amplitude of the optical field $E^0(t) = 10^5$ V/m, and $\tau_1 = 100$ fs[47].

First note that the magnitude of the current is of the order of pA-nA which is within experimental reach. I^x is maximum when the polarization of light coincides with the polar axis and decreases monotonically as the polarization turns away towards the y-axis. I^y, on the other hand, is nonmonotonic; it is zero when the light polarization and the polar axis coincide, then rises to a maximum at 45^0 and then decreases to zero for light polarized perpendicular to the polar axis.

In ultrafast pulsed experiments, the THz radiation emitted by the currents can be analyzed to study the nonlinear optical response of the system without need of mechanical contact. In this scenario the system does no have time to decay and the response is determined by the laser pulse characteristics not by the momentum dissipation mechanism. The above results indicate that the crystal structure, the geometry of the setup and light polarization can be used to uniquely characterize the jerk current tensor components. Injection and shift currents has been reported in THz spectroscopy in various materials[24,27,28,60–62].

X. 3RD ORDER INJECTION CURRENT

An explicit calculation of η_3 is given in Appendix E. The result is Eq. 122. We defined $\Omega^{ad}_{nm} \equiv \Omega^{ad}_n - \Omega^{ad}_m$ as the difference of Berry vector potentials. The Berry potential is related to the Berry curvature by $\Omega^{ad}_n = \sum_e \epsilon_{ade}\Omega^e_n$.

The covariant derivative of r^d_{mn}/ω_{nm} is with respect to the gauge dependent r^d_{mn} (see for example Eq. D6). The product $r^b_{nm}r^c_{mn;a}$ is gauge invariant and hence its covariant derivative reduces to the standard derivative (see for example Eq. B1). To simplify notation we also defined

$$[O(b),P(c)] \equiv O(b)P(c) - O(c)P(b) \tag{125}$$
$$D_\pm(\omega_{nm},\omega) \equiv \delta(\omega_{nm}-\omega) \pm \delta(\omega_{nm}+\omega), \tag{126}$$

where O, P are arbitrary matrix elements which depend on the cartesian indices b, c. For example

$$[r^b_{nm},r^c_{mn}] \equiv r^b_{nm}r^c_{mn} - r^c_{nm}r^d_{mn}. \tag{127}$$

One can see that η_3 in Eq. 122 is manifestly antisymmetric under exchange of b, c. In addition, it is easy to show that $\eta_3^{abcd}(0,\omega,-\omega,0)$ is pure imaginary and satisfies $[\eta_3^{abcd}(0,\omega,-\omega,0)]^* = -\eta_3^{abcd}(0,\omega,-\omega,0) = \eta_3^{abcd}(0,-\omega,\omega,0)$. Similar to η_2 the antisymmetry in the b, c indices implies that η_3 vanishes for linearly polarized light. η_3 represents the current

$$\frac{d}{dt}J^{a(3)}_{3i} = 6\sum_{bcd}\eta_3^{abcd}(0,\omega,-\omega,0)E^b(\omega)E^c(-\omega)E^d_0, \tag{128}$$

which varies as

$$|\mathbf{J}^{(3)}_{3i}| \sim \eta_3 t, \tag{129}$$

in the absence of momentum relaxation and saturation effects.

A. Materials

In general, the 81 components of η_3 are finite in both centrosymmetric and noncentrosymmetry crystal structures. In practice, the symmetries of the 32 crystal classes greatly reduce the number of independent components. For example, GaAs has $\bar{4}3m$ point group, with 21 nonzero components and 4 independent components.[38] However, η_3 is antisymmetric under exchange of b, c which reduces the number of independent components to 1. In 2D materials the number of components of η_3 is also small. For example, single-layer GeS has $mm2$ point group which contains a mirror-plane symmetry and a 2-fold axis. In this case η_3 has only 2 independent components.

In general, circular or unpolarized light will produce 3rd order injection current along the direction of the static field. Current transverse to the static field may not be generated with unpolarized or linear polarization.

B. Physical interpretation of 3rd order injection current

The presence of a static field gives rise to new physical processes which we now describe in detail.

1st term.- The first term in Eq.(122) arises from the asymmetric injection of carriers in anomalous velocity states. To see this, let us consider an electron wavepacket in band n subject to a static field E^d_0. The static field induces an anomalous contribution to the electron's ve-

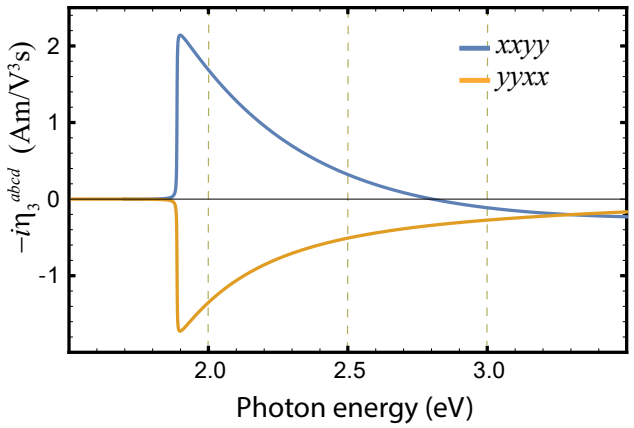

FIG. 5. Injection current response tensor η_3^{abcd} in single-layer GeS near the band edges. η_3 gives rise to current transverse to the static field. As can seen it will vanishes for linearly polarized light. The tight-binding model parameters are described in Sec. IX F.

locity which generates a current given by (Eq. 54)

$$\mathbf{J}_{3i,1} = -\frac{e^2}{\hbar V}\sum_{n\mathbf{k}} f_n \mathbf{E}_0 \times \mathbf{\Omega}_n, \tag{130}$$

where we used $f_n = \rho^{(0)}_{nn}$. Taking a time derivative of the occupations we obtain (to 2nd order in the optical field and 1st in the static field)

$$\frac{d}{dt}\mathbf{J}_{3i,1} = -\frac{e^2}{\hbar V}\sum_{n\mathbf{k}} \frac{df_n}{dt} \mathbf{E}_0 \times \mathbf{\Omega}_n. \tag{131}$$

This expression means that when the optical field is turned on electrons will be excited from the valence into anomalous conduction states. To lowest order in the intensity, Fermi's Golden rule gives the one-photon injection rate shown in Eq.(86). Using Eqs.(86) we obtain

$$\frac{d}{dt}J^{a(3)}_{3i,1} = -\frac{2\pi e^4}{\hbar^3}\sum_{b'c'd}\sum_{vc\mathbf{k}} \Omega^{ad}_{cv} r^{b'}_{cv} r^{c'}_{vc} \delta(\omega_{cv}-\omega)\times E^{b'}(\omega)E^{c'}(-\omega)E^d_0. \tag{132}$$

Using the fact that $\omega > 0$ we can extend the sum to all bands and recover the 1st term in Eq. 122.

2nd term.- In the presence of a static field a wavepacket drifts in the BZ giving rise to a current. Similarly, a dipole of two wavepackets drift in the presence of a static field giving rise to a current. To see this, consider the dipole velocity contribution to the current in Eq. 91. Writing explicitly the small imaginary part of the external frequencies and taking the resonant we obtain

$$J^{a(2)}_{3i,2} = -\frac{i\pi e^3}{\hbar^2 V}\sum_{bc}\sum_{nm\mathbf{k}} f_{nm}\big[r^b_{nm;a} r^c_{mn}\delta(\omega_{mn}+\omega) + r^c_{nm;a} r^b_{mn}\delta(\omega_{mn}-\omega)\big]E^b(\omega)E^c(-\omega). \tag{133}$$

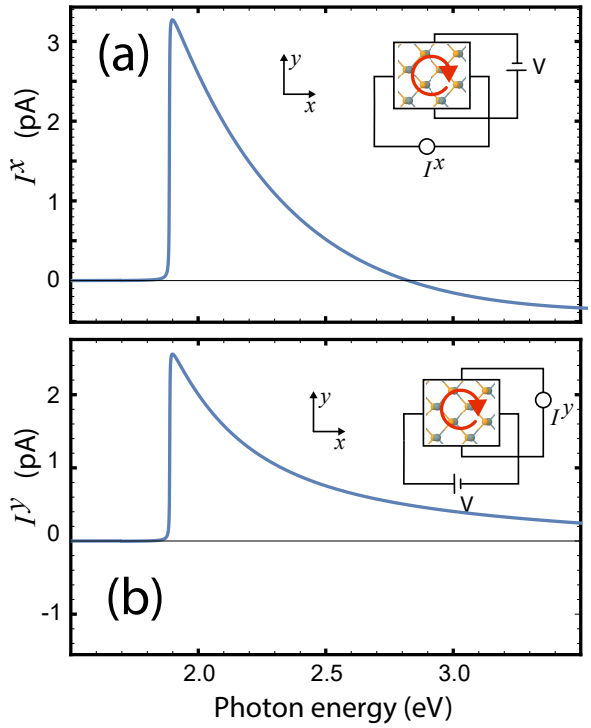

FIG. 6. η_3-Iinjection current in single-layer GeS near the band edge. (a) shows I^x and (b) I^b. Light is circularly polarized and incident perpendicular to the plane of the GeS. Two bias setups are shown.

Taking a time derivative of the dipole matrix elements, exchanging n, m indices and making $\mathbf{k} \to -\mathbf{k}$, we obtain

$$\frac{d}{dt}J^{a(3)}_{3i,2} = -\frac{i\pi e^4}{\hbar^3 V}\sum_{bcd}\sum_{nm\mathbf{k}} f_{nm}\frac{\partial}{\partial k^d}\big(r^b_{nm;a}r^c_{mn} - r^c_{nm;a}r^b_{mn}\big)\delta(\omega_{nm}-\omega)E^b(\omega)E^c(-\omega)E^d_0, \tag{134}$$

which can be recognized as the 2nd term in Eq. 122.

3rd term.- The 3rd term takes into account the change of the electron distribution due to the static field. To see this, let us consider the current of an electron wavepacket in band n to third order in the electric field. From Eq. 54

$$J^{a(3)}_{3i,3} = \frac{e}{V}\sum_{n\mathbf{k}} v^a_n \rho^{(3)}_{nn}. \tag{135}$$

Taking a time derivative of the density matrix gives

$$\frac{d}{dt}J^{a(3)}_{3i,3} = \frac{e}{V}\sum_{n\mathbf{k}} v^a_n \frac{\partial \rho^{(3)}_{nn}}{\partial t}. \tag{136}$$

From Eq. 58 the time derivative of the density matrix is

$$\frac{\partial \rho^{(3)}_{nn}}{\partial t} = \frac{e}{i\hbar}\sum_{bm} E^b(\rho^{(2)}_{nm}r^b_{mn} - r^b_{nm}\rho^{(2)}_{mn}) - \frac{e}{\hbar}\sum_b E^b \rho^{(2)}_{nn;b}. \tag{137}$$

Now consider the intraband part of the second order density matrix obtained from Eq. 63

$$\rho^{(2)}_{nm,intra} = \frac{ie}{\hbar}\sum_{b\beta c\sigma}\frac{\bar{\rho}^{(1)b\beta}_{nm;c}}{\omega_{mn}-\omega_\Sigma}E^b_\beta E^c_\sigma e^{-i\omega_\Sigma t}, \tag{138}$$

where $\omega_\Sigma = \omega_\beta + \omega_\sigma$. The first order density matrix in the presence of a static field is (see Eq. 61)

$$\bar{\rho}^{(1)d0}_{nm} = \frac{e}{\hbar}f_{mn}\frac{r^d_{nm}}{\omega_{nm}}. \tag{139}$$

Substituting the above equations into Eq. 137 and taking the resonant part we recover the 3rd term in Eq. 122. The factor of two in Eq. 122 is due to two possible choices for the static electric field.

4th term.- This contribution arises from electrons excited from the valence to conduction bands via an intermediate state l. These new states are generated by the presence of static field.

C. 3rd order injection Hall current

Let us assume a static field is in the x-direction and compute the current in the y-direction. An optical field of the form $\mathbf{E} = \hat{\mathbf{x}}E^x(\omega)e^{-i\omega t} + \hat{\mathbf{y}}E^y(\omega)e^{-i\omega t} + c.c.$ is incident perpendicular to the sample surface which we take to define the xy-plane. From Eq. 128 the current transverse to the static field is

$$\frac{d}{dt}J^{y(3)}_{3iH} = \varsigma^{yx}_{3iH}E^x_0 \tag{141}$$

where $E^a(\omega) = |E^a(\omega)|e^{-i\phi_a}$ and the Hall coefficient is

$$\varsigma^{yx}_{3iH} \equiv 12i\eta^{yyxx}_3|E^x(\omega)||E^y(\omega)|\sin(\phi_x-\phi_y). \tag{142}$$

Similar to η_2, η_3 vanishes for linear polarization $\phi_x = \phi_y$ and is maximum for circularly polarized light. In a simple relaxation time approximation, the dc singularity in the conductivity (see Eq. 97) is cut-off by a phenomenological relaxation time τ_1 as

$$\frac{\eta_3}{-i\omega_\Sigma} \to \frac{\eta_3}{\frac{1}{\tau_1}-i\omega_\Sigma}. \tag{143}$$

The current is

$$J^{y(3)}_{3iH} = \frac{\tau_1}{1-i\omega_\Sigma\tau_1}\varsigma^{yx}_{3iH}E^x_0, \tag{144}$$

If $\omega_\Sigma = 0$, the current is proportional to τ_1 the relaxation of the diagonal density matrix elements. For frequencies larger than the Drude peak $\omega_\Sigma\tau_1 \gg 1$ but smaller than interband transitions the current is independent of the scattering time and hence is a measure of the geometry of the Bloch wavefunctions.

D. Example: 3rd order injection current in single-layer GeS

To get a sense of the η_3-injection current in real materials we now calculate it for single-layer GeS. We use the same 2-band, 2D tight-binding model of single-layer GeS and same sample geometry as in Sec. IX F.

Out of the 16 tensor components the antisymmetry in the b, c indices and the mirror symmetry $y \to -y$ of the model leaves only two independent components, $yyxx$ and $xxyy$. This means that the current flows only perpendicular to the static electric.

These tensor components are shown in Fig. 5. The 2nd term in η_3 is the dominant term followed by the 3rd, and the 1st which are one and two orders of magnitude smaller respectively.

For concretes the optical field has circular polarization and the static field is along the polar (x-) axis of the sample as

$$\mathbf{E}(t) = \hat{\mathbf{x}}E^0(\omega)e^{-i\omega t} + \hat{\mathbf{y}}E^0(\omega)e^{-i\omega t} + c.c., \tag{145}$$

$$\mathbf{E}_0 = \hat{\mathbf{x}}E^x_0, \text{ or } \hat{\mathbf{y}}E^y_0, \tag{146}$$

where $\phi_x - \phi_y = \pi/2$. The transverse currents are given by

$$I^{x(3)}_{3i} = 12A\tau_1 i\eta^{xxyy}_3|E^x(\omega)||E^y(\omega)|E^x_0\sin(\phi_y-\phi_x) \tag{147}$$

$$I^{y(3)}_{3i} = 12A\tau_1 i\eta^{yyxx}_3|E^x(\omega)||E^y(\omega)|E^x_0\sin(\phi_x-\phi_y) \tag{148}$$

where $A = Ld$ is the transverse area of the sample. Note that the current vanishes for linearly polarized light but is maximum for circular polarization.

The calculated total induced current is shown in Fig. 6. The static field is shown in two configurations, namely, parallel and perpendicular to the polar axis of single-layer GeS. In both configurations the chirality of light is the same. The induced current is of the order of pA which is within experimental reach.

XI. 3RD ORDER SHIFT CURRENT

Explicit calculation of σ_3 gives Eq. 140. For details see Appendix F. In Eq. 140 we defined the anticummutator with respect to the b, c indices only as

$$\{O(b), P(c)\} \equiv O(b)P(c) + O(c)P(b) \tag{149}$$

where O, P are arbitrary matrix elements For example

$$\{\left(\frac{r^d_{mn}}{\omega_{nm}}\right)_{;c}, r^b_{nm;a}\} \equiv \left(\frac{r^d_{mn}}{\omega_{nm}}\right)_{;c} r^b_{nm;a} + \left(\frac{r^d_{mn}}{\omega_{nm}}\right)_{;b} r^c_{nm;a}. \tag{150}$$

$$\sigma_3^{abcd}(0,\omega,-\omega,0) = \frac{\pi e^4}{6\hbar^3 V}\sum_{nm\mathbf{k}} f_{mn}\left[\{\left(\frac{r^d_{mn}}{\omega_{nm}}\right)_{;c}, r^b_{nm;a}\} - \{\left(\frac{r^d_{mn;a}}{\omega_{nm}}\right)_{;c}, r^b_{nm}\}\right]\delta(\omega_{nm}-\omega)$$
$$- \frac{i\pi e^4}{6\hbar^3 V}\sum_{nml\mathbf{k}} \frac{f_{ln}}{\omega_{mn}}\left[\{r^c_{nl},(r^d_{mn}r^b_{lm})_{;a}\} - r^d_{mn}\{r^c_{nl;a}, r^b_{lm}\}\right] D_+(\omega_{nl},\omega). \tag{140}$$

D_+ is defined in Eq. 126. Clearly, σ_3 is symmetric under exchange of b,c, pure real, and satisfies $\sigma_3^{abcd}(0,\omega,-\omega,0) = \sigma_3^{acbd}(0,-\omega,\omega,0)$. The tensor defines the nonlinear current

$$J^{a(3)}_{sh} = 6\sum_{bcd}\sigma_3^{abcd}(0,\omega,-\omega,0)E^b(\omega)E^c(-\omega)E^d_0, \tag{151}$$

which, in the absence of momentum relaxation and saturation effects is constant with illumination time. Note that this calculation assumes quantum coherance in the solid.

A. Materials

In general, the 81 components of σ_3 are finite in both centrosymmetric and noncentrosymmetry crystal structures. In practice, the symmetries of the 32 crystal classes greatly reduce the number of independent components. For example, GaAs has $\bar{4}3m$ point group, with 21 nonzero components and 4 independent components[38]. However, σ_3 is antisymmetric under exchange of b,c which reduces the number of independent components to 3. In 2D materials the number of components of σ_3 is also small. For example, single-layer GeS has $mm2$ point group which contains a mirror-plane symmetry and a 2-fold axis. In this case σ_3 has only 6 independent components.

In general, linear, circular or unpolarized light will produce 3rd order shift current along the direction of the static field. Current transverse to the static field may not be generated with unpolarized or circular polarization.

B. Physical interpretation of the 3rd order shift current

1st term.- The first term in σ_3 arises from the quantum interference of dipole and band coherence oscillations. To see this, note that an oscillating external field creates an oscillating dipole which couples two distinct bands. The dipole velocity is given by Eq. 55. If the occupations of the bands oscillate 180^0 out of phase with respect to the dipole oscillations a dc (dipole) current can be established. The process is mediated by the intraband part of the (second order) density matrix as

$$J^{a(3)}_{3sh,1} = -\frac{e^2}{\hbar V}\sum_{nm\mathbf{k}} \mathbf{E}(t)\cdot\mathbf{r}_{nm;a}\rho^{(2)}_{mn,i}(t), \tag{152}$$

where $\rho^{(2)}_{mn,i}$ is the first term in Eq. 63 which clearly represents the intraband part of $\rho^{(2)}_{mn}$. Setting one of the fields in $\rho^{(2)}$ to be static (say $E^d_\delta \to E^d_0$) we have

$$J^{a(3)}_{3sh,1} = -\frac{ie^4}{\hbar^3 V}\sum_{b\beta c\sigma d}\sum_{nm\mathbf{k}} \frac{r^b_{nm;a}}{\omega_{mn}-\omega_\sigma}\left(\frac{r^d_{mn}f_{nm}}{\omega_{mn}}\right)_{;c} \times E^b_\beta E^c_\sigma E^d_0 e^{-i\omega_\Sigma t} \tag{153}$$

where $\omega_\Sigma = \omega_\beta + \omega_\sigma$. Symmetrizing with respect electric field indices, substituting $\omega_\beta = \pm\omega$ and $\omega_\sigma = \mp\omega$, and keeping only resonant terms we recover the 1st term in Eq. 140.

2nd term.- The second term in σ_3 arises from the quantum interference band coherence oscillations only. To see this, note that a static external field creates a static dipole which couples two distinct bands. The static dipole together with a static occupation of the bands create a dc (dipole) current. This process is also mediated by the (static) intraband part of the (second order) density matrix as

$$J^{a(3)}_{3sh,2} = -\frac{e^2}{\hbar V}\sum_{d}\sum_{nm\mathbf{k}} E^d_0 r^d_{nm;a}\rho^{(2)}_{mn,i}. \tag{154}$$

Following the same procedure as above and after an integration by parts it is easy to show that we recover the 2nd term in Eq. 140.

3rd and 4th term.- The 3rd and 4th terms in σ_3 are not easily derived from a simple model. These processes involve virtual transitions to intermediate bands created by the static external field and involve the interband part of the second order density matrix.

C. 3rd order shift Hall current

Let us assume a static field is in the x-direction and compute the shift current in the y-direction. An optical field of the form $\mathbf{E} = \hat{\mathbf{x}}E^x(\omega)e^{-i\omega t} + \hat{\mathbf{y}}E^y(\omega)e^{-i\omega t} + c.c.$ is incident perpendicular to the sample surface which we

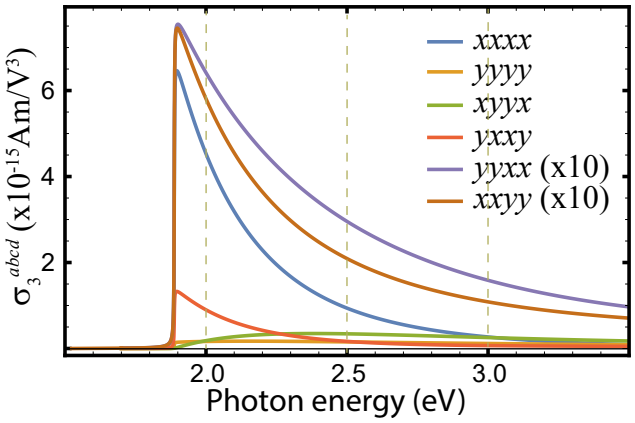

FIG. 7. Shift current response tensor σ_3^{abcd} of single-layer GeS near the band edges. The model parameters are the same as in Sec. IX F. The largest response is along the polarization axis x. The transverse response governed by $xxyy$ and $yyxx$ is an order of magnitude smaller.

take as the xy-plane. The current transverse to the static field is

$$J^{y(3)}_{3shH} = \varsigma^{yx}_{3shH} E^x_0 \tag{155}$$

where $E^a(\omega) = |E^a(\omega)|e^{-i\phi_a}$ and the effective Hall conductivity is

$$\varsigma^{yx}_{3shH} \equiv 12\sigma_3^{yyxx}|E^x(\omega)||E^y(\omega)|\cos(\phi_x - \phi_y). \tag{156}$$

Similar to σ_2, σ_3 vanishes for circular polarization and is maximum for linear polarization $\phi_x = \phi_y$ at 45^0 with respect to the x-axis. Contrary to injection current, the shift current does not have a Drude-like dc divergence but rather gives a finite contribution in this limit. Hence we expect that while quantum coherence is maintained in the solid the current is given by the above equation.

D. Example: 3rd order shift current in single-layer GeS

To get a sense of the 3rd order shift current in real materials we now calculate it for single-layer GeS. We use the same setup and tight-binding model of single-layer GeS as in Sec. IX F.

Because of the mirror symmetry $y \to -y$ of the model, only six tensor components are independent. As seen in Fig. 7, the strongest is along the polar axis of magnitude $\sim 5 \times 10^{-15}$ Am/V^3. The component transverse to the static electric field σ_3^{yyxx} (see Sec. XI C) is an order of magnitude smaller.

The sample is rectangular of dimensions $L \times L$ and thickness $d = 2.56$ Å and is biased by an external battery of voltage V as seen in Fig. 2c. For concreteness let us assume the optical field is incident perpendicularly to the

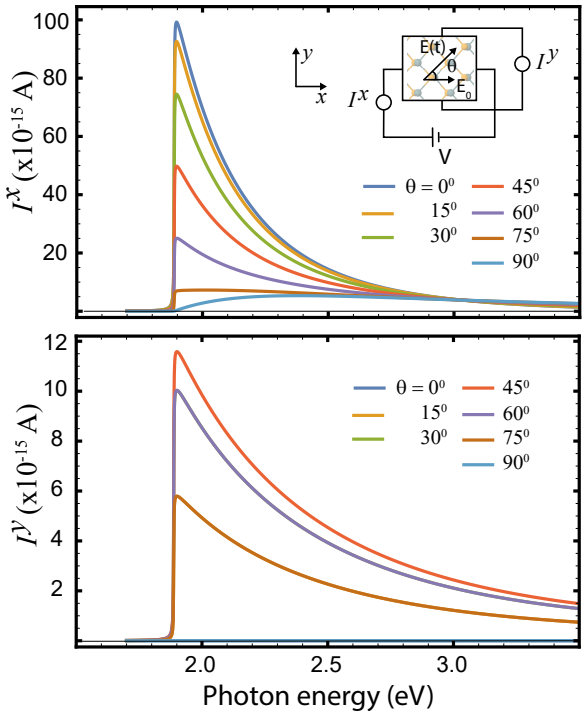

FIG. 8. σ_3-shift current in single-layer GeS near the band edge. (a) shows I^x and (b) I^y. Light is linearly polarized at an angle θ with respect to the polar axis (x-axis see inset).

plane of single-layer GeS as

$$\mathbf{E}(t) = \hat{\mathbf{x}}E^x(\omega)e^{-i\omega t} + \hat{\mathbf{y}}E^y(\omega)e^{-i\omega t} + c.c., \tag{157}$$
$$\mathbf{E}_0 = \hat{\mathbf{x}}E^x_0. \tag{158}$$

The longitudinal and transverse currents are

$$I^{x(3)}_{sh} = 6A(\sigma_3^{xxxx}|E^x(\omega)|^2 + \sigma_3^{xyyx}|E^y(\omega)|^2)E^x_0 \tag{159}$$
$$I^{y(3)}_{sh} = 6A\sigma_3^{yyxx}|E^x(\omega)||E^y(\omega)|\cos(\phi_x - \phi_y)E^x_0 \tag{160}$$

where $E^x(\omega) = E^0(\omega)\cos\theta e^{-i\phi_x}$, $E^y(\omega) = E^0(\omega)\sin\theta e^{-i\phi_y}$, θ is the angle with the x-axis, and $A = Ld$ is the transverse area of the sample. Note that the current along the polar x-axis is independent of the polarization of light and hence, it will not vanish even for unpolarized light. The transverse component of the current, on the other hand, vanishes for circularly polarized (and unpolarized) light and is maximum for linearly polarized light.

We chose the optical field linearly polarized ($\phi_x = \phi_y$) at an angle θ with the polar axis as shown in the inset to Fig. 8. The figure shows the total current along x and y-axis induced as a function of θ. We assumed the same semiconductor parameters as before, e.g., $L = 100\mu$m, $V = 1$V, $E^x_0 = V/L = 10^4$ V/m, amplitude of the optical field $E^0(t) = 10^5$ V/m, and $\tau_1 = 100$ fs.

First note that the magnitude of the currents is of the order of pA-fA. I^x is maximum when the polarization of

light coincides with the polar axis and decreases monotonically as the polarization turns away towards the y-axis. I^y, on the other hand, is nonmonotonic: it is zero when the polarization and the polar axis coincide, then rises to a maximum at 45^0 and then decreases to zero again for light polarized perpendicular to the polar axis.

XII. GENERALIZATIONS

A. Snap current

By power counting it is easy to see that the leading divergence of χ_4 is of order ω_Σ^{-4}, and that it occurs when all but two of the external frequencies are zero. Proceeding as before we calculate the corresponding response tensor $\varsigma_4^{abcde}(0,\omega,-\omega,0,0)$. Taking three derivatives of Eq. 84 and using Eqs. 86,112, and 113 we obtain

$$\begin{aligned}\varsigma_4^{abcde} = \frac{2\pi e^5}{4!\hbar^4 V}\sum_{nm\mathbf{k}} f_{mn}\big[&3\omega_{nm;ade}r^b_{nm}r^c_{mn}\\ &+3\omega_{nm;ad}(r^b_{nm}r^c_{mn})_{;e}\\ &+\omega_{nm;a}(r^b_{nm}r^c_{mn})_{;de}\big]\delta(\omega_{nm}-\omega).\end{aligned} \tag{161}$$

The tensor is symmetric in the b,c indices and represents a third derivative of the nonlinear current

$$\frac{d^3J^{a(4)}_{sp}}{dt^3} = 4!\sum_{bcde}\varsigma_4^{abcde}(0,\omega,-\omega,0,0)E^b(\omega)E^c(-\omega)E^d_0E^e_0, \tag{162}$$

where E^d_0, E^e_0 represent static fields. By analogy with a particle's third derivative of its velocity we dub it *snap* current. The current grows as $\sim t^3$ with illumination time in the absence of momentum relaxation and saturation effects. Hence, it is proportional the third power of the relaxation time τ_1

$$J^{a(4)}_{sp} = \tau_1^3 4!\sum_{bcde}\varsigma_4^{abcde}E^b(\omega)E^c(-\omega)E^d_0E^e_0. \tag{163}$$

Note that the snap current could be thought of a second order correction of the dark conductivity due to the presence of the optical field.

B. Higher order singularities

One can show that the leading physical divergence of χ_{ni} represents, in general, the $n-1$-th time derivative of a current and that these occur when all but two of the external frequencies are set to zero. They are obtained from the leading term in the Taylor expansions

$$(-i\omega_\Sigma)^4\chi_{3i} = \iota_3 + (-i\omega_\Sigma)\eta_3 + (-i\omega_\Sigma)^2\sigma_3 + ... \tag{164}$$
$$(-i\omega_\Sigma)^4\chi_{4i} = \varsigma_4 + (-i\omega_\Sigma)\iota_4 + (-i\omega_\Sigma)^2\eta_4 + ... \tag{165}$$
$$(-i\omega_\Sigma)^5\chi_{5i} = \kappa_5 + (-i\omega_\Sigma)\varsigma_5 + (-i\omega_\Sigma)^2\iota_5 + \cdots \tag{166}$$
$$(-i\omega_\Sigma)^6\chi_{6i} = \varpi_6 + (-i\omega_\Sigma)\kappa_6 + (-i\omega_\Sigma)^2\varsigma_6 + \cdots. \tag{167}$$
$$\vdots$$

These higher order analogs of the injection current are named by analogy to a particle's time derivatives of its velocity, e.g.,*jerk*, *snap*, *crackle*, *pop*,...,etc. and denote them by, ι, ς, κ, ϖ,.. respectively. Their physical origin is similar to the injection current namely the rate of carrier injection at current carrying states at time-reserved points in the BZ is asymmetric creating a polar distribution. The charges are then accelerated by the external field.

An alternative formulation is the Laurent series for χ_{ni} (or χ_n since χ_{ne} ir regular) as

$$\chi_{ni} = \sum_{l=-n}^{\infty} a_l z^l \tag{168}$$

where $z=-i\omega_\Sigma$ and $a_l=0$ for frequencies less than the gap. The residues $a_{-1}=\eta$, $a_{-2}=\sigma$, $a_{-3}=\iota$, etc., are formally given by

$$a_l = \frac{1}{2\pi i}\oint_{|z|=\rho}\frac{\chi_{ni}\,dz}{z^{l+1}}, \tag{169}$$

ρ is the radius of convergence of the $1/z$ series. In these calculations the limit $\rho\to 0$ is taken before the limit $\epsilon\to 0$.

In general, if more than two frequencies are distinct[32,39,63] (but $\omega_\Sigma=0$), the series starts from $l>-n$.

XIII. EXPERIMENTAL SIGNATURES

In real materials, the measured current will be limited by momentum dissipation mechanisms due to collisions with other electrons, phonons, or impurities. For weak disordered insulators we expect the dc divergence of the conductivity in Eq. 97 will be cut-off by a relaxation time constant as

$$\sigma^{(3)} = \frac{\iota_3}{(\frac{1}{\tau_1}-i\omega_\Sigma)^2} + \frac{\eta_3}{\frac{1}{\tau_1}-i\omega_\Sigma} + \sigma_3 + \cdots \tag{170}$$

Note that σ_3 relies on quantum coherence and hence its current will decay on the coherence time scale of the solid τ_2. Calculation of τ_2 requires a microscopic model of dissipation which will be presented elsewhere.

We have estimated the current of each contribution assuming that we can detect its signatures separately. This is a challenge in itself as is well documented in the

TABLE II. Summary of nonlinear Hall-like responses of single-layer GeS. A static electric field is present along the $x-$axis. In addition, an optical electric field is incident perpendicular to the plane of the sample which defines the xy-plane. The Hall current is in the y-axis. The sample geometry is shown in Fig. 2c and the details are in Sec. IX F. Polar axis of single-layer GeS defines the x-axis. I $\equiv$ inversion symmetry, no I $\equiv$ no inversion symmetry. Order of magnitude of current are given for frequencies near the band edge. I^x is the current along the x-axis. *For comparison, longitudinal current is given for η_2 and σ_2 for the same parameters. w.r.t. stands for with respect to.

Current I^y	Momentum relaxation	Dependence on E_0^x	I vs. no I	Hall current dependence on polarization	Hall current vanishes for polarization	Hall current maximum for polarization	Sign of I^x, I^y	Hall current magnitude*	Ref. Eq.
ι_3-jerk	τ_1^2	linear	I, no I	$\cos(\phi_x - \phi_y)$	circular, linear $\mathbf{E}(t) \parallel x, y$	linear at 45^0 w.r.t. x-axis	+,-	10^{-8} A	124
η_3-injection	τ_1	linear	I, no I	$\sin(\phi_x - \phi_y)$	linear	circular	+,+	10^{-12} A	148
σ_3-shift	τ_2	linear	I, no I	$\cos(\phi_x - \phi_y)$	circular, linear $\mathbf{E}(t) \parallel x, y$	linear at 45^0 w.r.t. x-axis	+,+	10^{-14} A	160
η_2-injection	τ_1	No	no I					10^{-6} A*	
σ_2-shift	τ_2	No	no I					10^{-8} A*	

literature[31]. Here we propose to use ultrafast THz spectroscopy together with the symmetry of the crystal, the geometry of the setup and the polarization of light to isolate these components. In ultrafast experiments, momentum relaxation plays a minor role and the magnitude of the current is given by the parameters of the lasers. For example the shift current magnitude follows the envelope of the pulse[24–27]. Recently, the 2nd order injection, shift or both currents have been reported via THz radiation[24–28,60–62]. In Table II we present a summary of the jerk, injection and shift Hall current component for a model of single-layer of GeS near the band edge. As we can see, either the dependence on polarization, the linearity of the static field, the order of magnitude of the induced current, or the momentum dissipation dependence can be used to distinguish them apart.

The jerk and σ_3-shift Hall currents have τ_1^2, τ_2 dependence momentum relaxation time scale. But, measuring this dependence can be difficult in THz experiments[27,28,60–62]. Since they have the same dependence on the polarization of light, the tie can be broken by the signs of the longitudinal vs transverse currents as shown in the 8th column of Table. II.

XIV. CONCLUSIONS

The 2nd order injection and shift currents are archetypical examples of nontrivial carrier dynamics in insulators and semiconductors. In this paper we revisited the derivation of the intraband current and proposed a microscopic interpretation of shift current based on the coherent motion of pairs of wavepackets.

We also studied the photocurrents to 2nd order in an optical and to 1st order in a static field from the perspective of the third order electric polarization susceptibility dc divergence. Three new bulk photovoltaic effects are found. We dub them jerk, 3rd order injection and 3rd order shift currents, respectively. The jerk current and 3rd order injection currents can be thought of as a higher order versions of the standard 2nd order injection current and have essentially the same microscopic origin, namely, the asymmetric rate of population of current-carrying states at time-reversed points in the BZ. The presence of the electric field, however, give rise the new contributions which are absent in the 2nd order injection current such as the anomalous and dipole velocity states.

The 3rd order shift current can be thought as a higher order version of the 2nd order shift current. It involves the coherent motion of pairs of wavepackets across the BZ. We showed that all photocurrents can be understood physically using semiclassical wavepacket dynamics. We have shown that generalizations to higher orders are possible and gave an example. Explicit expressions for the photocurrents amenable for first-principles computations are given. Estimates for single-layer GeS show that experimental observation of these currents is possible.

XV. ACKNOWLEDGMENTS

We thank J.E. Sipe, R.A. Muniz, Y. Lin and C. Aversa for useful discussions. We acknowledge support from DOE-NERSC Contract No. DE-AC02-05CH11231.

Appendix A: List of identities

Some definitions used in this paper are:

$$\mathbf{v}_{nn}(\mathbf{k}) = \langle u_n|\mathbf{v}|u_n\rangle \equiv \mathbf{v}_n(\mathbf{k}) \tag{A1}$$
$$f_n \equiv f(\epsilon_n(\mathbf{k})) \tag{A2}$$
$$f_{nm} \equiv f_n - f_m \tag{A3}$$
$$\boldsymbol{\xi}_{nm}(\mathbf{k}) \equiv i\,\langle u_n|\boldsymbol{\nabla}_{\mathbf{k}}|u_m\rangle \tag{A4}$$
$$\mathbf{r}_{nm}(\mathbf{k}) \equiv \boldsymbol{\xi}_{nm}(\mathbf{k}), \quad (m \neq n) \tag{A5}$$
$$\mathbf{r}_{nn}(\mathbf{k}) \equiv 0. \tag{A6}$$
$$\omega_{nm} \equiv \omega_n - \omega_m. \tag{A7}$$

They describe velocity matrix elements (A1), Fermi distribution (A2), Fermi function differences (A3), Berry connection (A4) , off-diagonal (A5) and diagonal dipole matrix elements (A6), respectively, and frequency band differences (A7). u_n is the periodic part of the Bloch wave function (spinor index contracted), and the covariant derivative of the dipole matrix elements is defined as

$$\mathbf{r}_{nm;a} \equiv \left[\frac{\partial}{\partial k^a} - i(\xi^a_{nn} - \xi^a_{mm})\right]\mathbf{r}_{nm}, \tag{A8}$$

or generally of any Bloch matrix element O_{nm} as

$$O_{nm;b} \equiv \left[\frac{\partial}{\partial k^b} - i(\xi^b_{nn} - \xi^b_{mm})\right]O_{nm}. \tag{A9}$$

We also defined the commutator and anticommutator with respect to the Cartesian indices b, c as

$$[O(b), K(c)] \equiv O(b)K(c) - O(c)K(b) \tag{A10}$$
$$\{O(b), K(c)\} \equiv O(b)K(c) + O(c)K(b) \tag{A11}$$

where O, K are any Bloch matrix elements. Some identities used in this paper:

$$\omega_n(-\mathbf{k}) = \omega_n(\mathbf{k}) \tag{A12}$$
$$\omega_{n;a}(-\mathbf{k}) = -\omega_{n;a}(\mathbf{k}) = -\frac{\partial}{\partial k^a}\omega_n(\mathbf{k}) \tag{A13}$$
$$\mathbf{v}_{nm}(-\mathbf{k}) = -\mathbf{v}_{mn}(\mathbf{k}) = -[\mathbf{v}_{nm}(\mathbf{k})]^* \tag{A14}$$
$$\mathbf{r}_{nm}(-\mathbf{k}) = \mathbf{r}_{mn}(\mathbf{k}) = (\mathbf{r}_{mn}(-\mathbf{k}))^* \tag{A15}$$
$$\mathbf{r}_{nm;a}(-\mathbf{k}) = -\mathbf{r}_{mn;a}(\mathbf{k}) = -(\mathbf{r}_{nm;a}(\mathbf{k}))^* \tag{A16}$$
$$\omega_{nm;a}(\mathbf{k}) = v^a_n(\mathbf{k}) - v^a_m(\mathbf{k}) = -\omega_{nm;a}(-\mathbf{k}) = \omega_{mn;a}(-\mathbf{k}) \tag{A17}$$
$$\boldsymbol{\Omega}_n(-\mathbf{k}) = -\boldsymbol{\Omega}_n(\mathbf{k}) = -(\boldsymbol{\Omega}_n(\mathbf{k}))^*. \tag{A18}$$

They arise from the hermicity of operators and the assumptions of time-reversal invariance of the ground state. $\hbar\omega_n$ and $\boldsymbol{\Omega}_n$ denote the band energy and Berry curvature of band n.

Appendix B: Derivation of η_2 and σ_2 from Taylor expansion of χ_2

To compute $\eta_2^{abc}(0,\omega,-\omega)$ and $\sigma_2^{abc}(0,\omega,-\omega)$ from Eq. 4, start from Eq. 70 and symmetrize $(-i\omega_\Sigma)^2\chi_{2i}$ with respect to pair-wise exchanges of electric fields indices b,β and c,σ[38]. Then write explicitly the small imaginary part of frequencies, $\omega_\beta \to \omega_\beta + i\epsilon$, $\omega_\sigma \to \omega_\sigma + i\epsilon$ and let $1/(x-i\epsilon) = 1/x + i\pi\delta(x)$. Next, set $\omega_\beta = \omega + n_\beta\omega_\Sigma, \omega_\sigma = -\omega + n_\sigma\omega_\Sigma$, $1 = n_\beta + n_\sigma$, and Taylor expand real parts up to first order in ω_Σ. It is easy to show that the non-resonant terms cancel and we obtain Eq. 75 and 78 as claimed. In this calculation we used

$$\begin{aligned}(r^c_{nm}r^b_{mn})_{;a} &= r^c_{nm;a}r^b_{mn} + r^c_{nm}r^b_{mn;a}\\ &= \frac{\partial}{\partial k^a}(r^c_{nm}r^b_{mn})\end{aligned} \tag{B1}$$

and some identities listed in Appendix A. Note that the expression $r^c_{nm}r^b_{mn}$ is gauge invariant and hence the covariant derivative reduces to the standard crystal momentum derivative.

Appendix C: Expansion of χ_{3i}

Using Eqs. 37, 54, 63, and 66 the third order susceptibility $\chi_3^{abcd}(-\omega_\Sigma,\omega_\beta,\omega_\sigma,\omega_\Delta)$ can be written as $\chi_3 = \chi_{3e} + \chi_{3i}$ where

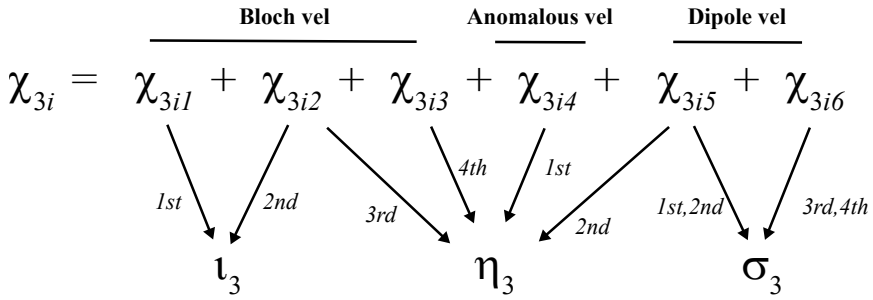

FIG. 9. Origin of the $1st, 2nd, ...$ contributions to the expressions for ι_3-jerk (Eq. 107), η_3-injection (Eq. 122) and σ_3-shift (Eq. 140) response tensors. Each of the 6 terms in the χ_{3i} originates from either the Bloch velocity (first three), anomalous velocity (4th) and the dipole velocity (5th and 6th). Due to the structure of the poles in these expressions shift current processes also contribute to injection processes as shown by the 2nd term in η_3.

$$\begin{aligned}\frac{\chi_{3e}}{C_3} =& -\sum_{nm\mathbf{k}} \frac{r^a_{nm}}{\omega_{mn}-\omega_\Sigma}\left[\frac{1}{(\omega_{mn}-\omega_2)}\left(\frac{r^b_{mn}f_{nm}}{\omega_{mn}-\omega_\beta}\right)_{;c}\right]_{;d} - i\sum_{nmp\mathbf{k}} \frac{r^a_{nm}}{\omega_{mn}-\omega_\Sigma}\left[\frac{1}{\omega_{mn}-\omega_2}\left(\frac{r^b_{mp}r^c_{pn}f_{pm}}{\omega_{mp}-\omega_\beta}-\frac{r^c_{pm}r^b_{pn}f_{np}}{\omega_{pn}-\omega_\beta}\right)\right]_{;d}\\ &-i\sum_{nmp\mathbf{k}} \frac{r^a_{nm}}{\omega_{mn}-\omega_\Sigma}\left[\left(\frac{r^b_{mp}f_{pm}}{\omega_{mp}-\omega_\beta}\right)_{;c}\frac{r^d_{pn}}{\omega_{mp}-\omega_2}-\frac{r^b_{mp}}{\omega_{pn}-\omega_2}\left(\frac{r^b_{pn}f_{np}}{\omega_{pn}-\omega_\beta}\right)_{;c}\right]\\ &-\sum_{nmpl\mathbf{k}} \frac{r^a_{nm}}{\omega_{mn}-\omega_\Sigma}\left[\frac{r^d_{mp}}{\omega_{pn}-\omega_2}\left(\frac{r^b_{pl}r^c_{lp}f_{lp}}{\omega_{pl}-\omega_\beta}-\frac{r^c_{pl}r^b_{ln}f_{nl}}{\omega_{lp}-\omega_\beta}\right)-\left(\frac{r^b_{ml}r^c_{lp}f_{lm}}{\omega_{ml}-\omega_\beta}-\frac{r^c_{ml}r^b_{lp}f_{pl}}{\omega_{lp}-\omega_\beta}\right)\frac{r^d_{pn}}{\omega_{mp}-\omega_2}\right]\end{aligned} \tag{C1}$$

$$\begin{aligned}\frac{\chi_{3i}}{C_3} \equiv& \sum_{r=1}^{6}\chi_{3ir}\\ =& \frac{1}{\omega_2\omega_\Sigma^2}\sum_{nm\mathbf{k}}\omega_{nm;a}f_{mn}\left(\frac{r^b_{nm}r^c_{mn}}{\omega_{nm}-\omega_\beta}\right)_{;d}\\ &-\frac{1}{\omega_\Sigma^2}\sum_{nm\mathbf{k}}\frac{\omega_{nm;a}r^d_{mn}}{\omega_{nm}-\omega_2}\left(\frac{r^b_{nm}f_{mn}}{\omega_{nm}-\omega_\beta}\right)_{;c}-\frac{i}{\omega_\Sigma^2}\sum_{nml\mathbf{k}}\frac{\omega_{nm;a}r^d_{mn}}{\omega_{nm}-\omega_2}\left(\frac{r^b_{nl}r^c_{lm}f_{ln}}{\omega_{nl}-\omega_\beta}-\frac{r^c_{nl}r^b_{lm}f_{ml}}{\omega_{lm}-\omega_\beta}\right)\\ &-\frac{i}{\omega_2\omega_\Sigma}\sum_{nm\mathbf{k}}\Omega^{ad}_{nm}\frac{r^b_{nm}r^c_{mn}f_{mn}}{\omega_{nm}-\omega_\beta}\\ &+\frac{1}{\omega_\Sigma}\sum_{nm\mathbf{k}}\frac{r^d_{mn;a}}{\omega_{nm}-\omega_2}\left(\frac{r^b_{nm}f_{mn}}{\omega_{nm}-\omega_\beta}\right)_{;c}+\frac{i}{\omega_\Sigma}\sum_{nml\mathbf{k}}\frac{r^d_{mn;a}}{\omega_{nm}-\omega_2}\left(\frac{r^b_{nl}r^c_{lm}f_{ln}}{\omega_{nl}-\omega_\beta}-\frac{r^c_{nl}r^b_{lm}f_{ml}}{\omega_{lm}-\omega_\beta}\right).\end{aligned} \tag{C2}$$

We defined $C_3 \equiv e^4/\hbar^3 V$, $\Omega^{ad}_{nm} \equiv \Omega^{ad}_n - \Omega^{ad}_m$, $\omega_\Sigma \equiv \omega_\beta + \omega_\sigma + \omega_\Delta$ and $\omega_2 = \omega_\beta + \omega_\sigma$. These expressions still need to be symmetrized with respect to pair-wise exchange of electric field indices (b,β), (c,σ), (d,Δ). It is easier to calculate χ_{3i} is calculated from the intraband current rather than from $\mathbf{P}^{(3)}_i$.

Eq. C2 has a distinguishable structure, see Fig 9. The first three terms in χ_{3i} are derived from the combination $v^a_n\rho^{(3)}_{nn}$ (Eq. 54). By analogy with χ_{2i} (Eq. 70), we would expect these terms to be injection current-type of contributions with one caveat; the 1st term has no analog in χ_{2i} since it is proportional to *three* powers of frequency, $\omega_\Sigma^{-2}\omega_2^{-1}$ and is the most divergent at zero frequency. The second and third terms, proportional to ω_Σ^{-2}, seem stan-

dard injection coefficients similar to the 1st term in χ_{2i}.

The 4th term is proportional to $(\omega_\Sigma\omega_2)^{-1}$ and arises from the anomalous velocity $(\mathbf{E}\times\mathbf{\Omega})^a\rho^{(2)}_{nn}$. It is an injection current-type of coefficient. The fifth and sixth terms, proportional to ω_Σ^{-1}, originate from $\mathbf{E}\cdot\mathbf{r}_{nm;a}\rho^{(2)}_{mn}$ and hence are expected to be shift current-type of contributions.

The goal in the next sections is to calculate the coefficients $\iota_3, \eta_3, \sigma_3$ in the expansion

$$(-i\omega_\Sigma)^3\chi_{3i} = \iota_3 + (-i\omega_\Sigma)\eta_3 + (-i\omega_\Sigma)^2\sigma_3 + \cdots \quad \text{(C3)}$$

To avoid cumbersome notation in the next three sections (D,E,F) we write the susceptibilities with the additional factors as

$$\frac{(-i\omega_\Sigma)^3\chi^{abcd}_{3i}}{C_3} \to \chi_{3i} \quad \text{(C4)}$$

The strategy is to parametrize (the real part of) the external frequencies as

$$\begin{aligned}\omega_\beta &= \omega + n_\beta\omega_\Sigma,\\ \omega_\sigma &= -\omega + n_\sigma\omega_\Sigma,\\ \omega_\Delta &= 0,\end{aligned} \quad \text{(C5)}$$

subject to $n_\beta + n_\sigma = 1$. Fig. 9 summarize the result.

Appendix D: Derivation of ι_3

ι_3 derives from χ_{3i1} and χ_{3i2}.

1. 1st term of ι_3

Integrate by parts χ_{3i1} and symmetrize it with respect to pair-wise exchange of electric field indices (b,β), (c,σ), (d,Δ) [38] to obtain

$$\begin{aligned}\chi_{3i,1} &\equiv \sum_{l=1}^{3}\chi_{3i,1,l}\\ &= -\frac{i\omega_\Sigma}{6}\sum_{nm\mathbf{k}}\frac{\omega_{nm;ad}f_{mn}r^b_{nm}r^c_{mn}}{(\omega_{nm}-\omega_\beta)(\omega_{nm}+\omega_\sigma)}\\ &\quad -\frac{i\omega_\Sigma}{6}\sum_{nm\mathbf{k}}\frac{\omega_{nm;ac}f_{mn}r^b_{nm}r^d_{mn}}{(\omega_{nm}-\omega_\beta)(\omega_{nm}+\omega_\Delta)}\\ &\quad -\frac{i\omega_\Sigma}{6}\sum_{nm\mathbf{k}}\frac{\omega_{nm;ab}f_{mn}r^d_{nm}r^c_{mn}}{(\omega_{nm}-\omega_\Delta)(\omega_{nm}+\omega_\sigma)}\end{aligned} \quad \text{(D1)}$$

The 2nd and 3rd terms will cancel against other terms as we show later, but the first term will contribute to ι_3. By partial fractions and writing explicitly the imaginary parts of the frequencies, the first term gives

$$\begin{aligned}\chi_{3i,1,1} &= \frac{-i\omega_\Sigma}{6(\omega_\beta+\omega_\sigma)}\sum_{nm\mathbf{k}}\frac{\omega_{nm;ad}f_{mn}r^b_{nm}r^c_{mn}}{(\omega_{nm}-\omega_\beta-i\epsilon)}\\ &\quad -\frac{i\omega_\Sigma}{6(\omega_\beta+\omega_\sigma)}\sum_{nm\mathbf{k}}\frac{\omega_{nm;ad}f_{mn}r^c_{nm}r^b_{mn}}{(\omega_{nm}-\omega_\sigma-i\epsilon)}.\end{aligned} \quad \text{(D2)}$$

Using Eq. C5, $1/(x-i\epsilon) = 1/x + i\pi\delta(x)$, and expanding in powers of ω_Σ to 1st order we obtain

$$\begin{aligned}\chi_{3i,1,1} &= \frac{2\pi}{6}\sum_{nm\mathbf{k}}\omega_{nm;ad}f_{mn}r^b_{nm}r^c_{mn}\delta(\omega_{nm}-\omega)\\ &\quad -\frac{i\omega_\Sigma}{6}\sum_{nm\mathbf{k}}\omega_{nm;ad}f_{mn}r^b_{nm}r^c_{mn}\frac{\partial}{\partial\omega}\left(\frac{1}{\omega_{nm}-\omega}\right)\end{aligned} \quad \text{(D3)}$$

The first term is independent of ω_Σ and vanishes for frequencies smaller than the energy band gap. This is the first term of ι_3 in Eq. 107. The second nonresonant term will cancel against other terms.

2. 2nd term of ι_3

This contribution is obtained from χ_{3i2}. To see this, let us symmetrize the 2nd term in Eq. C2. After two integration by parts we obtain

$$\chi_{3i2} \equiv \sum_{l=1}^{8} \chi_{3i2,l} = \frac{i\omega_\Sigma}{6} \sum_{nm\mathbf{k}} \frac{\omega_{nm;ac} r^d_{mn} r^b_{nm} f_{mn}}{(\omega_{nm}-\omega_\beta-\omega_\sigma)(\omega_{nm}-\omega_\beta)} + \frac{i\omega_\Sigma}{6} \sum_{nm\mathbf{k}} \frac{\omega_{nm;a} r^b_{nm} f_{mn}}{\omega_{nm}-\omega_\beta} \left(\frac{r^d_{mn}}{\omega_{nm}-\omega_\beta-\omega_\sigma}\right)_{;c}$$
$$+ \frac{i\omega_\Sigma}{6} \sum_{nm\mathbf{k}} \frac{\omega_{nm;ab} r^d_{mn} r^c_{nm} f_{mn}}{(\omega_{nm}-\omega_\beta-\omega_\sigma)(\omega_{nm}-\omega_\sigma)} + \frac{i\omega_\Sigma}{6} \sum_{nm\mathbf{k}} \frac{\omega_{nm;a} r^c_{nm} f_{mn}}{\omega_{nm}-\omega_\sigma} \left(\frac{r^d_{mn}}{\omega_{nm}-\omega_\beta-\omega_\sigma}\right)_{;b}$$
$$- \frac{i\omega_\Sigma}{6} \sum_{nm\mathbf{k}} \frac{\omega_{nm;a} r^c_{mn} f_{mn}}{\omega_{nm}-\omega_\beta-\omega_\Delta} \left(\frac{r^b_{nm}}{\omega_{nm}-\omega_\beta}\right)_{;d} - \frac{i\omega_\Sigma}{6} \sum_{nm\mathbf{k}} \frac{\omega_{nm;a} r^b_{mn} f_{mn}}{\omega_{nm}-\omega_\Delta-\omega_\sigma} \left(\frac{r^d_{nm}}{\omega_{nm}-\omega_\Delta}\right)_{;c}$$
$$- \frac{i\omega_\Sigma}{6} \sum_{nm\mathbf{k}} \frac{\omega_{nm;a} r^b_{mn} f_{mn}}{\omega_{nm}-\omega_\sigma-\omega_\Delta} \left(\frac{r^c_{nm}}{\omega_{nm}-\omega_\sigma}\right)_{;d} - \frac{i\omega_\Sigma}{6} \sum_{nm\mathbf{k}} \frac{\omega_{nm;a} r^c_{mn} f_{mn}}{\omega_{nm}-\omega_\Delta-\omega_\beta} \left(\frac{r^d_{nm}}{\omega_{nm}-\omega_\Delta}\right)_{;b}. \quad \text{(D4)}$$

There are 8 terms. To $\mathcal{O}(\omega_\Sigma)$, the $l = 1, 3$ terms cancel with identical 2nd and 3rd terms in Eq. D1. The terms $l = 2, 6$ and $l = 4, 8$ combine to give the third term of η_3 in Eq. 122 (see next section). The $l = 5, 7$ terms contribute to ι_3.

Note that we can set $\omega_\beta + \omega_\sigma = 0$ (or $\omega_\Delta = 0$) (where this combination appears) since the pair of poles of the expression are distinct. This is not true in $l = 5, 7$ and we consider them separately. After differentiation the $l = 5$ term we obtain

$$\chi_{3i2,5} = -\frac{i\omega_\Sigma}{6} \sum_{nm\mathbf{k}} \frac{\omega_{nm;a} r^c_{mn} r^b_{nm;d} f_{mn}}{(\omega_{nm}-\omega_2)(\omega_{nm}-\omega_\beta)}$$
$$+ \frac{i\omega_\Sigma}{6} \sum_{nm\mathbf{k}} \frac{\omega_{nm;a} r^c_{mn} r^b_{nm} f_{mn} \omega_{nm;d}}{(\omega_{nm}-\omega_2)(\omega_{nm}-\omega_\beta)^2} \quad \text{(D5)}$$

here $\omega_2 = \omega_\beta + \omega_\Delta$ and we used

$$\left(\frac{r^d_{nm}}{\omega_{nm}-\omega_\Delta}\right)_{;c} = \frac{r^d_{nm;c}}{\omega_{nm}-\omega_\Delta} - \frac{r^d_{nm}\omega_{nm;c}}{(\omega_{nm}-\omega_\Delta)^2}. \quad \text{(D6)}$$

Now obtain simple poles via partial fractions. The term with a square of frequencies in denominator can be handled by

$$\frac{\omega_{nm;d}}{(\omega_{nm}-\omega_\Delta)^2} = -\frac{\partial}{\partial k^d}(\omega_{nm}-\omega_\beta)^{-1} \quad \text{(D7)}$$

and a partial integration. Next, write the imaginary part of frequencies, use $1/(x-i\epsilon) = 1/x + i\pi\delta(x)$, and set $\omega_\beta = \omega + n_\beta\omega_\Sigma, \omega_\sigma = -\omega + n_\sigma\omega_\Sigma$, and $1 = n_\beta + n_\sigma$. Note that with these definitions $\omega_2 = \omega + (1+n_\beta)\omega_\Sigma$. Now expand to *second* order in ω_Σ and set (without expanding) $\omega_\Delta = \omega_\Sigma$. After some algebra we obtain

$$\chi_{3i2,5} = \frac{i\omega_\Sigma}{6} \sum_{nm\mathbf{k}} r^c_{mn} r^b_{nm;d} f_{mn} \frac{\partial}{\partial k^a}\left(\frac{1}{\omega_{nm}-\omega}\right)$$
$$+ \frac{i\omega_\Sigma}{12} \sum_{nm\mathbf{k}} \frac{\partial}{\partial k^d}(\omega_{nm;a} r^c_{mn} r^b_{nm}) f_{mn} \frac{\partial}{\partial\omega}\left(\frac{1}{\omega_{nm}-\omega}\right)$$
$$+ \frac{\pi}{6} \sum_{nm\mathbf{k}} \frac{\partial}{\partial k^d}(\omega_{nm;a} r^c_{mn} r^b_{nm}) f_{mn} \delta(\omega_{nm}-\omega) \quad \text{(D8)}$$

In this calculation we have used the identity

$$\frac{\partial}{\partial\omega}\left(\frac{1}{\omega_{nm}-\omega}\right) = -\frac{\partial}{\partial\omega_{nm}}\left(\frac{1}{\omega_{nm}-\omega}\right). \quad \text{(D9)}$$

Note that the 3rd term in (D8) contributes to ι_3. The other two nonresonant terms which will eventually cancel. A similar calculation for the $l = 7$ terms gives

$$\chi_{3i2,7} = \frac{i\omega_\Sigma}{6} \sum_{nm\mathbf{k}} r^b_{mn} r^c_{nm;d} f_{mn} \frac{\partial}{\partial k^a}\left(\frac{1}{\omega_{nm}+\omega}\right)$$
$$- \frac{i\omega_\Sigma}{12} \sum_{nm\mathbf{k}} \frac{\partial}{\partial k^d}(\omega_{nm;a} r^b_{mn} r^c_{nm}) f_{mn} \frac{\partial}{\partial\omega}\left(\frac{1}{\omega_{nm}+\omega}\right)$$
$$+ \frac{\pi}{6} \sum_{nm\mathbf{k}} \frac{\partial}{\partial k^d}(\omega_{nm;a} r^b_{mn} r^c_{nm}) f_{mn} \delta(\omega_{nm}+\omega) \quad \text{(D10)}$$

Combining the $l = 5$ and $l = 7$ terms above and using B1 we obtain

$$\chi_{3i2,5} + \chi_{3i2,7} =$$
$$\frac{i\omega_\Sigma}{6} \sum_{nm\mathbf{k}} \omega_{nm;ad} r^c_{mn} r^b_{nm} f_{mn} \frac{\partial}{\partial\omega}\left(\frac{1}{\omega_{nm}-\omega}\right)$$
$$+ \frac{2\pi}{6} \sum_{nm\mathbf{k}} \frac{\partial}{\partial k^d}(\omega_{nm;a} r^c_{mn} r^b_{nm}) f_{mn} \delta(\omega_{nm}-\omega) \quad \text{(D11)}$$

The 1st term is nonresonant and will cancel against the 2nd term in Eq. D3. The 2nd term combined with the first term in Eq. D3 gives ι_3 in Eq. 107.

Appendix E: Derivation of η_3

We now derive each of the contributions to η_3 in Eq. 122.

1. 1st term of η_3

The first term in η_3 comes from χ_{3i4}. Symmetrizing χ_{3i4} in Eq. D4 and after partial fractions we obtain

$$\chi_{3i,4} \equiv \sum_{l=1}^{3} \chi_{3i,4,l} \tag{E1}$$
$$= \frac{\omega_\Sigma^2}{6(\omega_\beta+\omega_\sigma)} \sum_{nm\mathbf{k}} \Omega^{ad}_{nm} f_{mn} r^b_{nm} r^c_{mn} \left[\frac{1}{\omega_{nm}-\omega_\beta} - \frac{1}{\omega_{nm}+\omega_\sigma} \right]$$
$$+ \frac{\omega_\Sigma^2}{6} \sum_{nm\mathbf{k}} \frac{\Omega^{ac}_{nm} f_{mn} r^b_{nm} r^d_{mn}}{(\omega_{nm}-\omega_\beta)(\omega_{nm}+\omega_\Delta)}$$
$$+ \frac{\omega_\Sigma^2}{6} \sum_{nm\mathbf{k}} \frac{\Omega^{ab}_{nm} f_{mn} r^d_{nm} r^c_{mn}}{(\omega_{nm}-\omega_\Delta)(\omega_{nm}+\omega_\sigma)} \tag{E2}$$

Only the 1st term contributes to η_3. Writing the imaginary parts of the frequencies, setting $\omega_\beta = \omega + n_\beta \omega_\Sigma$, $\omega_\sigma = -\omega + n_\sigma \omega_\Sigma$, and Taylor expanding, we obtain to leading order in ω_Σ

$$\chi_{3i,4,1} = \frac{2i\pi\omega_\Sigma}{6} \sum_{nm\mathbf{k}} \Omega^{ad}_{nm} f_{mn} r^b_{nm} r^c_{mn} \delta(\omega_{nm}-\omega)$$
$$+ \frac{\omega_\Sigma^2}{6} \sum_{nm\mathbf{k}} \Omega^{ad}_{nm} f_{mn} r^b_{nm} r^c_{mn} \frac{\partial}{\partial\omega}\left(\frac{1}{\omega_{nm}-\omega}\right) \tag{E3}$$

Adding 1/2 of the first term to 1/2 of itself and letting $\mathbf{k} \to -\mathbf{k}$ in the 2nd term we obtain the first contribution of η_3 in Eq. 122. The 2nd term cancels against other nonresonant contributions.

2. 2nd term of η_3

This term arises from χ_{3i5}. Symmetrizing we obtain

$$\chi_{3i5} \equiv \sum_{l=1}^{6} \chi_{3i5,l} = \frac{i\omega_\Sigma^2}{6} \sum_{nm\mathbf{k}} \frac{r^d_{mn;a} f_{mn}}{\omega_{nm}-\omega_\beta-\omega_\sigma} \left(\frac{r^b_{nm}}{\omega_{nm}-\omega_\beta}\right)_{;c} + \frac{i\omega_\Sigma^2}{6} \sum_{nm\mathbf{k}} \frac{r^d_{mn;a} f_{mn}}{\omega_{nm}-\omega_\beta-\omega_\sigma} \left(\frac{r^c_{nm}}{\omega_{nm}-\omega_\sigma}\right)_{;b}$$
$$+ \frac{i\omega_\Sigma^2}{6} \sum_{nm\mathbf{k}} \frac{r^c_{mn;a} f_{mn}}{\omega_{nm}-\omega_\beta-\omega_\Delta} \left(\frac{r^b_{nm}}{\omega_{nm}-\omega_\beta}\right)_{;d} + \frac{i\omega_\Sigma^2}{6} \sum_{nm\mathbf{k}} \frac{r^b_{mn;a} f_{mn}}{\omega_{nm}-\omega_\Delta-\omega_\sigma} \left(\frac{r^d_{nm}}{\omega_{nm}-\omega_\Delta}\right)_{;c}$$
$$+ \frac{i\omega_\Sigma^2}{6} \sum_{nm\mathbf{k}} \frac{r^b_{mn;a} f_{mn}}{\omega_{nm}-\omega_\sigma-\omega_\Delta} \left(\frac{r^c_{nm}}{\omega_{nm}-\omega_\sigma}\right)_{;d} + \frac{i\omega_\Sigma^2}{6} \sum_{nm\mathbf{k}} \frac{r^c_{mn;a} f_{mn}}{\omega_{nm}-\omega_\Delta-\omega_\delta} \left(\frac{r^d_{nm}}{\omega_{nm}-\omega_\Delta}\right)_{;b}. \tag{E4}$$

Let us consider $\chi_{3i5,3}$ first

$$\chi_{3i5,3} = \frac{i\omega_\Sigma^2}{6} \sum_{nm\mathbf{k}} \frac{r^c_{mn;a} f_{mn}}{\omega_{nm}-\omega_2} \left(\frac{r^b_{nm}}{\omega_{nm}-\omega_\beta}\right)_{;d}, \tag{E5}$$

where $\omega_2 = \omega_\beta + \omega_\Delta$. Performing a partial fraction expansion, a substitution $1/(x-i\epsilon) = 1/x + i\pi\delta(x)$, followed by a Taylor expansion (to 2nd order) in ω_Σ of the real part about $(\omega_\beta, \omega_2) = (\omega, \omega)$ using $\omega_\beta = \omega + n_\beta\omega_\Sigma, \omega_\sigma = -\omega + n_\sigma\omega_\Sigma$ such that $\omega_2 = \omega + (1+n_\beta)\omega_\Sigma$, we obtain

$$\chi_{3i5,3} = \frac{i\omega_\Sigma^2}{6} \sum_{nm\mathbf{k}} r^c_{mn;a} r^b_{nm;d} f_{mn} \frac{\partial}{\partial\omega}\left(\frac{1}{\omega_{nm}-\omega}\right)$$
$$- \frac{i\omega_\Sigma^2}{12} \sum_{nm\mathbf{k}} (r^c_{mn;a} r^b_{nm})_{;d} f_{mn} \frac{\partial}{\partial\omega}\left(\frac{1}{\omega_{nm}-\omega}\right)$$
$$+ \frac{i\omega_\Sigma(i\pi)}{6} \sum_{nm\mathbf{k}} (r^c_{mn;a} r^b_{nm})_{;d} f_{mn} \delta(\omega_{nm}-\omega) \tag{E6}$$

the first two terms are nonresonant contributions which cancel against other terms. A similar analysis of $\chi_{3i5,5}$ gives

$$\chi_{3i5,5} = -\frac{i\omega_\Sigma^2}{6} \sum_{nm\mathbf{k}} r^b_{mn;a} r^c_{nm;d} f_{mn} \frac{\partial}{\partial\omega}\left(\frac{1}{\omega_{nm}+\omega}\right)$$
$$+ \frac{i\omega_\Sigma^2}{12} \sum_{nm\mathbf{k}} (r^b_{mn;a} r^c_{nm})_{;d} f_{mn} \frac{\partial}{\partial\omega}\left(\frac{1}{\omega_{nm}+\omega}\right)$$
$$+ \frac{i\omega_\Sigma(i\pi)}{6} \sum_{nm\mathbf{k}} (r^b_{mn;a} r^c_{nm})_{;d} f_{mn} \delta(\omega_{nm}+\omega) \tag{E7}$$

the first two terms are nonresonant contributions which cancel against other terms. After changing indices n, m and $\mathbf{k} \to -\mathbf{k}$ we see that the 3rd term in Eq. E6 plus the 3rd term in Eq. E7 gives the 2nd term of η_3 in Eq. 122.

3. 3rd term of η_3

The third contribution to Eq. 122 arise from $\chi_{3i2,2} + \chi_{3i2,6} + \chi_{3i2,4} + \chi_{3i2,8}$ in Eq. D4.

Note that we can set $\omega_\beta + \omega_\sigma = 0$ from the outset since the poles in these expressions are distinct. Setting $1/(x - i\epsilon) = 1/x + i\pi\delta(x)$ and Taylor expanding about $(\omega_\beta, \omega_\sigma) = (\omega, -\omega)$ we see that to leading order the non-resonant parts vanish and we obtain

$$\chi_{3i2,2} + \chi_{3i2,6} = -\frac{\omega_\Sigma \pi}{3} \sum_{bm\mathbf{k}} \omega_{nm;a} \left(\frac{r^d_{mn}}{\omega_{nm}}\right)_{;c} r^b_{nm} f_{mn} \delta(\omega_{nm} - \omega). \quad \text{(E8)}$$

Similar manipulations lead to vanishing nonresonant terms and to

$$\chi_{3i2,4} + \chi_{3i2,8} = -\frac{\omega_\Sigma \pi}{3} \sum_{bm\mathbf{k}} \omega_{nm;a} \left(\frac{r^d_{mn}}{\omega_{nm}}\right)_{;b} r^c_{nm} f_{mn} \delta(\omega_{nm} + \omega). \quad \text{(E9)}$$

Relabeling of indices n, m, setting $\mathbf{k} \to -\mathbf{k}$, and adding to Eq. E8 we recover the 3rd term of η_3.

4. 4th term of η_3

The 4th term arises from χ_{3i3}. Let us label the 12 terms obtained after symmetrization of χ_{3i3} as

$$\begin{aligned}
\chi_{3i3} &\equiv \sum_l^{12} \chi_{3i3,l} \\
&= \frac{\omega_\Sigma}{6} \sum_{nmo\mathbf{k}} \frac{\omega_{nm;a} r^d_{mn}}{\omega_{nm} - \omega_\beta - \omega_\sigma} \left[\frac{r^b_{no} r^c_{om} f_{on}}{\omega_{no} - \omega_\beta} - \frac{r^c_{no} r^b_{om} f_{mo}}{\omega_{om} - \omega_\beta}\right] + \frac{\omega_\Sigma}{6} \sum_{nmo\mathbf{k}} \frac{\omega_{nm;a} r^d_{mn}}{\omega_{nm} - \omega_\sigma - \omega_\beta} \left[\frac{r^c_{no} r^b_{om} f_{on}}{\omega_{no} - \omega_\sigma} - \frac{r^b_{no} r^c_{om} f_{mo}}{\omega_{om} - \omega_\sigma}\right] \\
&+ \frac{\omega_\Sigma}{6} \sum_{nmo\mathbf{k}} \frac{\omega_{nm;a} r^c_{mn}}{\omega_{nm} - \omega_\beta - \omega_\Delta} \left[\frac{r^b_{no} r^d_{om} f_{on}}{\omega_{no} - \omega_\beta} - \frac{r^d_{no} r^b_{om} f_{mo}}{\omega_{om} - \omega_\beta}\right] + \frac{\omega_\Sigma}{6} \sum_{nmo\mathbf{k}} \frac{\omega_{nm;a} r^b_{mn}}{\omega_{nm} - \omega_\Delta - \omega_\sigma} \left[\frac{r^d_{no} r^c_{om} f_{on}}{\omega_{no} - \omega_\Delta} - \frac{r^c_{no} r^d_{om} f_{mo}}{\omega_{om} - \omega_\Delta}\right] \\
&+ \frac{\omega_\Sigma}{6} \sum_{nmo\mathbf{k}} \frac{\omega_{nm;a} r^b_{mn}}{\omega_{nm} - \omega_\sigma - \omega_\Delta} \left[\frac{r^c_{no} r^d_{om} f_{on}}{\omega_{no} - \omega_\sigma} - \frac{r^d_{no} r^c_{om} f_{mo}}{\omega_{om} - \omega_\sigma}\right] + \frac{\omega_\Sigma}{6} \sum_{nmo\mathbf{k}} \frac{\omega_{nm;a} r^c_{mn}}{\omega_{nm} - \omega_\Delta - \omega_\beta} \left[\frac{r^d_{no} r^b_{om} f_{on}}{\omega_{no} - \omega_\Delta} - \frac{r^b_{no} r^d_{om} f_{mo}}{\omega_{om} - \omega_\Delta}\right].
\end{aligned} \quad \text{(E10)}$$

We analyze the structure of χ_{3i3} by dividing its terms into two groups. The first group composed of the $l = 1, 2, 3, 4$ terms can be added together to give a simple result (see Eq. E15). The second group is composed of the l = 5-12 terms. The $l = 5, 6, 9, 10$ terms have pair of poles separable by partial fractions and can be combined with the $l = 12, 11, 8, 7$ terms (respectively). Since we are interested in results to linear in ω_Σ, it is useful to note we can set $\omega_\beta + \omega_\sigma = 0$ or $\omega_\Delta = 0$ in all terms from the outset. This is because the pair of poles in each term are always distinct and separable by simple partial fractions. This should be contrasted with the $l = 5, 7$ terms of Eq. D4, or the l=3,5 terms in Eq. E4, where the poles collide and they have to be treated separately.

The sum of the $l = 1, 2$ terms can be written as

$$\chi_{3i3,1} + \chi_{3i3,2} = = \frac{\omega_\Sigma}{6} \sum_{nmo\mathbf{k}} \frac{\omega_{nm;a} r^d_{mn} r^b_{no} r^c_{om} f_{on}}{\omega_{nm}} F_+(\omega_{no}, \omega_\beta), \quad \text{(E11)}$$

where F_+ is defined as

$$\begin{aligned}
F_+(\omega_{no}, \omega_\beta) &\equiv \frac{1}{\omega_{no} - \omega_\beta - i\epsilon} + \frac{1}{\omega_{no} + \omega_\beta + i\epsilon} \\
&= H_+(\omega_{no}, \omega_\beta) + i\pi D_-(\omega_{no}, \omega_\beta),
\end{aligned} \quad \text{(E12)}$$

and

$$\begin{aligned}
H_\pm(\omega_{no}, \omega_\beta) &\equiv \frac{1}{\omega_{no} - \omega_\beta} \pm \frac{1}{\omega_{no} + \omega_\beta} \\
D_\pm(\omega_{no}, \omega_\beta) &\equiv \delta(\omega_{no} - \omega_\beta) \pm \delta(\omega_{no} + \omega_\beta).
\end{aligned} \quad \text{(E13)}$$

Similar manipulations for the sum of the $l = 3, 4$ terms leads to

$$\chi_{3i3,3} + \chi_{3i3,4} = = \frac{\omega_\Sigma}{6} \sum_{nmo\mathbf{k}} \frac{\omega_{nm;a} r^d_{mn} r^c_{no} r^b_{om} f_{on}}{\omega_{nm}} F_+(\omega_{no}, \omega_\sigma) \quad \text{(E14)}$$

Adding the l = 1-4 contributions we find

$$\sum_l^4 \chi_{3i3,l} =$$
$$= \frac{\omega_\Sigma}{6} \sum_{nmo\mathbf{k}} \omega_{nm;a} \frac{r^d_{mn}}{\omega_{nm}} (r^b_{no} r^c_{om} + r^c_{no} r^b_{om}) f_{on} H_+(\omega_{no}, \omega)$$
$$+ \frac{i\pi\omega_\Sigma}{6} \sum_{nmo\mathbf{k}} \omega_{nm;a} \frac{r^d_{mn}}{\omega_{nm}} (r^b_{no} r^c_{om} - r^c_{no} r^b_{om}) f_{on} D_-(\omega_{no}, \omega) \tag{E15}$$

The first term will cancel against other nonresonant contributions.

Next we consider the group of $l = 5, 6, 9, 10$. It is easy to show these terms can be written as

$$\chi_{3i3,5} \equiv \sum_l^4 \chi_{3i3,5,l} = \frac{\omega_\Sigma}{6} \sum_{nmo\mathbf{k}} \frac{\omega_{nm;a} r^c_{mn} r^b_{no} r^d_{om} f_{on}}{\omega_{mo}} \left[\frac{1}{\omega_{nm} - \omega} + i\pi\delta(\omega_{nm} - \omega) - \frac{1}{\omega_{no} - \omega} - i\pi\delta(\omega_{no} - \omega) \right], \tag{E16}$$

$$\chi_{3i3,6} \equiv \sum_l^4 \chi_{3i3,6,l} = \frac{\omega_\Sigma}{6} \sum_{nmo\mathbf{k}} \frac{\omega_{nm;a} r^c_{mn} r^d_{no} r^b_{om} f_{mo}}{\omega_{no}} \left[\frac{1}{\omega_{nm} - \omega} + i\pi\delta(\omega_{nm} - \omega) - \frac{1}{\omega_{om} - \omega} - i\pi\delta(\omega_{om} - \omega) \right], \tag{E17}$$

$$\chi_{3i3,9} \equiv \sum_l^4 \chi_{3i3,9,l} = \frac{\omega_\Sigma}{6} \sum_{nmo\mathbf{k}} \frac{\omega_{nm;a} r^b_{mn} r^c_{no} r^d_{om} f_{on}}{\omega_{mo}} \left[\frac{1}{\omega_{nm} + \omega} + i\pi\delta(\omega_{nm} + \omega) - \frac{1}{\omega_{no} + \omega} - i\pi\delta(\omega_{no} + \omega) \right], \tag{E18}$$

$$\chi_{3i3,10} \equiv \sum_l^4 \chi_{3i3,10,l} = \frac{\omega_\Sigma}{6} \sum_{nmo\mathbf{k}} \frac{\omega_{nm;a} r^b_{mn} r^d_{no} r^c_{om} f_{mo}}{\omega_{no}} \left[\frac{1}{\omega_{nm} + \omega} + i\pi\delta(\omega_{nm} + \omega) - \frac{1}{\omega_{om} + \omega} - i\pi\delta(\omega_{om} + \omega) \right]. \tag{E19}$$

We now combine them with the resonant (r) and nonresonant (nr) parts of the $l = 12, 11, 8, 7$ terms (respectively). The result is

$$\chi_{3i3,5,1} + (\chi_{3i3,12})_{nr} = -\frac{\omega_\Sigma}{6} \sum_{nmo\mathbf{k}} \frac{\omega_{nm;a} r^c_{mn} r^b_{no} r^d_{om} f_{mn}}{\omega_{om}(\omega_{nm} - \omega)}, \tag{E20}$$

$$\chi_{3i3,5,2} + (\chi_{3i3,12})_r = -\frac{i\pi\omega_\Sigma}{6} \sum_{nmo\mathbf{k}} \frac{\omega_{nm;a} r^c_{mn} r^b_{no} r^d_{om} f_{mn}}{\omega_{om}} \delta(\omega_{nm} - \omega), \tag{E21}$$

$$\chi_{3i3,6,1} + (\chi_{3i3,11})_{nr} = \frac{\omega_\Sigma}{6} \sum_{nmo\mathbf{k}} \frac{\omega_{nm;a} r^c_{mn} r^d_{no} r^b_{om} f_{mn}}{\omega_{no}(\omega_{nm} - \omega)}, \tag{E22}$$

$$\chi_{3i3,6,2} + (\chi_{3i3,11})_r = -\frac{i\pi\omega_\Sigma}{6} \sum_{nmo\mathbf{k}} \frac{\omega_{nm;a} r^c_{mn} r^d_{no} r^b_{om} f_{mn}}{\omega_{on}} \delta(\omega_{nm} - \omega), \tag{E23}$$

$$\chi_{3i3,9,1} + (\chi_{3i3,8})_{nr} = -\frac{\omega_\Sigma}{6} \sum_{nmo\mathbf{k}} \frac{\omega_{nm;a} r^b_{mn} r^c_{no} r^d_{om} f_{mn}}{\omega_{om}(\omega_{nm} + \omega)}, \tag{E24}$$

$$\chi_{3i3,9,2} + (\chi_{3i3,8})_r = -\frac{i\pi\omega_\Sigma}{6} \sum_{nmo\mathbf{k}} \frac{\omega_{nm;a} r^b_{mn} r^c_{no} r^d_{om} f_{mn}}{\omega_{om}} \delta(\omega_{nm} + \omega), \tag{E25}$$

$$\chi_{3i3,10,1} + (\chi_{3i3,7})_{nr} = \frac{\omega_\Sigma}{6} \sum_{nmo\mathbf{k}} \frac{\omega_{nm;a} r^b_{mn} r^d_{no} r^c_{om} f_{mn}}{\omega_{no}(\omega_{nm} + \omega)}, \tag{E26}$$

$$\chi_{3i3,10,2} + (\chi_{3i3,7})_r = \frac{i\pi\omega_\Sigma}{6} \sum_{nmo\mathbf{k}} \frac{\omega_{nm;a} r^b_{mn} r^d_{no} r^c_{om} f_{mn}}{\omega_{no}} \delta(\omega_{nm} + \omega). \tag{E27}$$

Now we want to show that to $\mathcal{O}(\omega_\Sigma)$ the resonant part of the sum of the l = 1-4 and l = 5-12 groups gives the

4th term of η_3 and the nonresonant part vanishes. First the resonant contributions.

a. *Resonant contributions*

Let $n \leftrightarrow m$ and $\mathbf{k} \to -\mathbf{k}$ in $\chi_{3i3,6,4}$ and add to $\chi_{3i3,5,4}$ to obtain

$$\chi_{3i3,6,4} + \chi_{3i3,5,4} = -\frac{i\pi\omega_\Sigma}{6} \sum_{nmo\mathbf{k}} \omega_{nm;a} \frac{r^c_{mn} r^d_{om} r^b_{no} f_{on}}{\omega_{mo}} D_-(\omega_{no}, \omega). \quad \text{(E28)}$$

Similar manipulations on $\chi_{3i3,10,4}$ and $\chi_{3i3,9,4}$ give

$$\chi_{3i3,10,4} + \chi_{3i3,9,4} = \frac{i\pi\omega_\Sigma}{6} \sum_{nmo\mathbf{k}} \omega_{nm;a} \frac{r^b_{mn} r^d_{om} r^c_{no} f_{on}}{\omega_{mo}} D_-(\omega_{no}, \omega). \quad \text{(E29)}$$

Adding Eq. E28 and E29 gives

$$\chi_{3i3,6,4} + \chi_{3i3,5,4} + \chi_{3i3,10,4} + \chi_{3i3,9,4} = \frac{i\pi\omega_\Sigma}{6} \sum_{nmo\mathbf{k}} \omega_{nm;a} \frac{r^d_{om}}{\omega_{mo}} (r^b_{mn} r^c_{no} - r^c_{mn} r^b_{no}) f_{on} D_-(\omega_{no}, \omega). \quad \text{(E30)}$$

Performing analogous manipulations add Eq. E21 to Eq. E23 and Eq. E25 to Eq. E27 to obtain

$$\chi_{3i3,5,2} + (\chi_{3i3,12})_r + \chi_{3i3,6,2} + (\chi_{3i3,11})_r = -\frac{i\pi\omega_\Sigma}{6} \sum_{nmo\mathbf{k}} \omega_{nm;a} \frac{r^c_{mn} r^b_{no} r^d_{om} f_{mn}}{\omega_{om}} D_-(\omega_{nm}, \omega), \quad \text{(E31)}$$

and

$$\chi_{3i3,10,2} + (\chi_{3i3,7})_r + \chi_{3i3,9,2} + (\chi_{3i3,8})_r = \frac{i\pi\omega_\Sigma}{6} \sum_{nmo\mathbf{k}} \omega_{nm;a} \frac{r^b_{mn} r^d_{om} r^c_{no} f_{mn}}{\omega_{om}} D_-(\omega_{nm}, \omega). \quad \text{(E32)}$$

respectively. After $n \leftrightarrow l$, and $\mathbf{k} \to -\mathbf{k}$ in Eq. E30 add to Eq. E15 to obtain

$$(\sum_l^4 \chi_{3i3,l})_r + \chi_{3i3,6,4} + \chi_{3i3,5,4} + \chi_{3i3,10,4} + \chi_{3i3,9,4} = \frac{i\pi\omega_\Sigma}{6} \sum_{nmo\mathbf{k}} \omega_{nl;a} \frac{r^d_{mn}}{\omega_{nm}} (r^b_{no} r^c_{om} - r^c_{no} r^b_{om}) f_{on} D_-(\omega_{no}, \omega). \quad \text{(E33)}$$

Now add Eq. E31 and Eq. E32 to obtain

$$\chi_{3i3,6,2} + (\chi_{3i3,11})_r + \chi_{3i3,5,2} + (\chi_{3i3,12})_r + \chi_{3i3,10,2} + (\chi_{3i3,7})_r + \chi_{3i3,9,2} + (\chi_{3i3,8})_r = \frac{i\pi\omega_\Sigma}{6} \sum_{nmo\mathbf{k}} \omega_{no;a} \frac{r^d_{mn}}{\omega_{nm}} (r^b_{no} r^c_{om} - r^c_{no} r^b_{om}) f_{on} D_-(\omega_{no}, \omega). \quad \text{(E34)}$$

Finally, the sum of all resonant terms in χ_{3i3} to linear order in ω_Σ amounts to adding Eq. E33 to Eq. E34. The result is

$$E33 + E34 = \frac{2i\pi\omega_\Sigma}{6} \sum_{nmo\mathbf{k}} \omega_{no;a} \frac{r^d_{mn}}{\omega_{nm}} (r^b_{no} r^c_{om} - r^c_{no} r^b_{on}) f_{on} D_-(\omega_{no}, \omega) \quad \text{(E35)}$$

which is the 4th term in η_3.

b. *Nonresonant contributions*

The sum the nonresonant third term of Eqs. E16, E17, E18 and E19 give

$$\chi_{3i3,6,3} + \chi_{3i3,5,3} + \chi_{3i3,9,3} + \chi_{3i3,10,3} = -\frac{\omega_\Sigma}{6} \sum_{nmo\mathbf{k}} \omega_{nm;a} \frac{r^d_{om} (r^c_{mn} r^b_{no} + r^b_{mn} r^c_{no}) f_{on}}{\omega_{mo}} H_+(\omega_{no}, \omega). \quad \text{(E36)}$$

Next, the sum of Eqs. E20 and E22 and of Eq. E24 and E26 gives

$$\chi_{3i3,5,1} + (\chi_{3i3,12})_{nr} + \chi_{3i3,6,1} + (\chi_{3i3,11})_{nr} = -\frac{\omega_\Sigma}{6} \sum_{nmo\mathbf{k}} \omega_{nm;a} \frac{r^c_{mn} r^b_{no} r^d_{om} f_{mn}}{\omega_{om}} H_+(\omega_{nm}, \omega), \quad \text{(E37)}$$

$$\chi_{3i3,9,1} + (\chi_{3i3,8})_{nr} + \chi_{3i3,10,1} + (\chi_{3i3,7})_{nr} = -\frac{\omega_\Sigma}{6} \sum_{nmo\mathbf{k}} \omega_{nm;a} \frac{r^b_{mn} r^c_{no} r^d_{om} f_{mn}}{\omega_{om}} H_+(\omega_{nm}, \omega). \quad \text{(E38)}$$

After $l \leftrightarrow n$ and $\mathbf{k} \to -\mathbf{k}$ in Eq. E36 combined with the nonresonant part of Eq. E15 we obtain

$$(\sum_l^4 \chi_{3i3,l})_{nr} + \chi_{3i3,6,3} + \chi_{3i3,5,3} + \chi_{3i3,9,3} + \chi_{3i3,10,3} = \frac{\omega_\Sigma}{6} \sum_{nmo\mathbf{k}} \omega_{no;a} \frac{r^d_{mn} (r^c_{om} r^b_{no} + r^b_{om} r^c_{no}) f_{on}}{\omega_{nm}} H_+(\omega_{no}, \omega). \quad \text{(E39)}$$

Adding Eq. E37 and Eq. E38 we obtain

$$E37 + E38 = -\frac{\omega_\Sigma}{6}\sum_{nmo\mathbf{k}} \omega_{nm;a}\frac{r^d_{om}(r^c_{no}r^b_{mn}+r^b_{no}r^c_{mn})f_{mn}}{\omega_{om}}H_+(\omega_{no},\omega), \tag{E40}$$

which after $l \leftrightarrow n$ and $n \leftrightarrow m$, is seen to cancel Eq. E39. This concludes the proof that to linear order on ω_Σ the nonresonant terms vanish.

Appendix F: Derivation of σ_3

1. 1st and 2nd terms in σ_3

Consider $\chi_{3i5,1}$ and $\chi_{3i5,2}$ in Eq.E4. In these terms we can set $\omega_\beta + \omega_\sigma = 0$ since the real part of the denominators never vanishes. Setting $1/(x - i\epsilon) = 1/x + i\pi\delta(x)$ and using

$$\frac{\partial}{\partial k^c}\left(\frac{r^d_{mn;a}r^b_{nm}}{\omega_{nm}}\right) = \left(\frac{r^d_{mn;a}}{\omega_{nm}}\right)_{;c} r^b_{nm} + \left(\frac{r^d_{mn;a}}{\omega_{nm}}\right) r^b_{nm;c} \tag{F1}$$

the resonant parts are

$$(\chi_{3i5,1}+\chi_{3i5,2})_r = \frac{\pi\omega_\Sigma^2}{6}\sum_{nm\mathbf{k}} f_{mn}\left[\left(\frac{r^d_{mn;a}}{\omega_{nm}}\right)_{;c} r^b_{nm} + \left(\frac{r^d_{mn;a}}{\omega_{nm}}\right)_{;b} r^c_{nm}\right]\delta(\omega_{nm}-\omega) \tag{F2}$$

Similar manipulations on $\chi_{3i5,4}$ and $\chi_{3i5,6}$ in Eq. E4 yield the rest of the terms in the square brackets in σ_3. The nonresonant parts can be shown to vanish.

2. 3rd and 4th terms in σ_3

This contributions to σ_3 arises from χ_{3i6} in Eq. C2. It can be shown that the nonresonant parts vanish and the resonant part gives the 3rd and 4th term in σ_3. Since the algebraic steps are very similar to those used in finding the third term in η_3 we omit the derivation.

Appendix G: two-band model of single-layer GeS

We consider a two-band, 2D model of single-layer GeS. The Hamiltonian is

$$H = f_0\sigma_0 + f_a\sigma_a, \tag{G1}$$

where $\sigma_a, a = x, y, z$ are the standard Pauli matrices and σ_0 is the 2×2 identity matrix. In this section, summation over repeated indices is implied. The functions f_a are given by the hopping integrals of the model. The Hamiltonian has eigenvectors given by

$$u_c = A\begin{pmatrix} f_x - if_y \\ \epsilon - f_z\end{pmatrix} \tag{G2}$$

$$u_v = A\begin{pmatrix} f_z - \epsilon \\ f_x + if_y\end{pmatrix}, \tag{G3}$$

where $A^{-2} = 2\epsilon(\epsilon - f_z)$ is the normalization and eigenvalues by $E_{c,v} = f_0 \pm \epsilon$ where $\epsilon = \sqrt{f_a f_a}$ and c, v denote the conduction and valence band respectively. An arbitrary phase factor has been omitted, since the final expressions are independent of this phase. The Bloch wave functions are constructed as

$$\psi_{n\mathbf{k}} = \sum_{\mathbf{R}} e^{i\mathbf{k}\cdot\mathbf{R}}[u^{(1)}_n\phi(\mathbf{r}-\mathbf{R}) + e^{i\mathbf{k}\cdot\mathbf{r}_0}u^{(2)}_n\phi(\mathbf{r}-\mathbf{r}_0-\mathbf{R})], \tag{G4}$$

where $u^{(i)}_n$ denotes the eigenvector corresponding to eigenvalue $n = v, c$ (valence, conduction) and $i = 1, 2$ denotes the first and second components. $\mathbf{r}_0 = (a_0, 0)$ is the position of site B with respect to site A which is taken to be the origin. $\phi(\mathbf{r})$ are p_z-orbitals and $\mathbf{R}$ runs over all lattice positions. Notice that the phase of the wave function at site B is different than that at site A.

The hopping parameters of the Hamiltonian are[56]

$$f_0 = 2t'_1[\cos\mathbf{k}\cdot\mathbf{a}_1 + \cos\mathbf{k}\cdot\mathbf{a}_2] + 2t'_2\cos\mathbf{k}\cdot(\mathbf{a}_1-\mathbf{a}_2), \tag{G5}$$

$$f_x - if_y = e^{i\mathbf{k}\cdot\mathbf{r}_0}(t_1 + t_2\Phi_{\mathbf{k}} + t_3\Phi^*_{\mathbf{k}}), \tag{G6}$$

$$f_z = \Delta, \tag{G7}$$

where $\Phi_{\mathbf{k}} \equiv e^{-i\mathbf{k}\cdot\mathbf{a}_1} + e^{-i\mathbf{k}\cdot\mathbf{a}_2}$, Δ is the onsite potential and $t_1, t_2, t_3, t'_1, t'_2$ are hopping matrix elements as indicated in Fig. 2(c). $\mathbf{a}_1 = (a_x, -a_y), \mathbf{a}_2 = (a_x, a_y)$ are the primitive lattice vectors. Note that f_0 and hence t'_1, t'_2 do not enter into the injection current.

For single-layer GeS the parameters are: $(a_x, a_y, d) = (4.53/2, 3.63/2, 2.56)$ Å, where d is the thickness of the slab, $a_0 = 0.62$ Å, and $(t_1, t_2, t_3, t'_1, t'_2, \Delta) = (-2.33, 0.61, 0.13, 0.07, -0.09, 0.41)$ eV. It was shown that these parameters reproduce the band structure and geometry of the wavefunction in the vicinity of the Gamma point[56]. To compare with bulk values the results are multiplied by $2/d$. The factor of 2 accounts for the smaller TB unit cell.

[1] R. Karplus and J. M. Luttinger, Phys. Rev. **95**, 1154 (1954).
[2] N. Nagaosa, J. Sinova, S. Onoda, A. H. MacDonald, and N. P. Ong, Rev. Mod. Phys. **82**, 1539 (2010).
[3] N. P. Armitage, E. J. Mele, and A. Vishwanath, Rev. Mod. Phys. **90**, 015001 (2018).
[4] A. Vishwanath, Physics **8**, 84 (2015).
[5] B. I. Sturman and V. M. Fridkin, *The Photovoltaic and Photorefractive Effects in Non-CentrosymmetricMaterials* (Gordon and Breach Science Publishers, Philadelphia, 1992).
[6] V. I. Belinicher and B. I. Sturman, Physics-Uspekhi **23**, 199 (1980).
[7] V. I. Belinicher and B. I. Sturman, Ferroelectrics **83**, 29 (1988).
[8] R. von Baltz and W. Kraut, Phys. Rev. B **23**, 5590 (1981).
[9] J. E. Spanier, V. M. Fridkin, A. M. Rappe, A. R. Akbashev, A. Polemi, Y. Qi, Z. Gu, S. M. Young, C. J. Hawley, D. Imbrenda, G. Xiao, A. L. Bennett-Jackson, and C. L. Johnson, Nature Photonics **10**, 611 (2016).
[10] A. M. Rappe, I. Grinberg, and J. E. Spanier, Proceedings of the National Academy of Sciences **114**, 7191 (2017).
[11] K. Kushnir, M. Wang, P. D. Fitzgerald, K. J. Koski, and L. V. Titova, ACS Energy Letters **2**, 1429 (2017).
[12] B. M. Fregoso, T. Morimoto, and J. E. Moore, Phys. Rev. B **96**, 075421 (2017).
[13] T. Rangel, B. M. Fregoso, B. S. Mendoza, T. Morimoto, J. E. Moore, and J. B. Neaton, Phys. Rev. Lett. **119**, 067402 (2017).
[14] J. E. Sipe and A. I. Shkrebtii, Phys. Rev. B **61**, 5337 (2000).
[15] D. H. Auston, A. M. Glass, and A. A. Ballman, Phys. Rev. Lett. **28**, 897 (1972).
[16] A. M. Glass, D. von der Linde, and T. J. Negran, Applied Physics Letters **25**, 233 (1974).
[17] W. T. H. Koch, R. Munser, W. Ruppel, and P. Wrfel, Ferroelectrics **13**, 305 (1976).
[18] C. Somma, K. Reimann, C. Flytzanis, T. Elsaesser, and M. Woerner, Phys. Rev. Lett. **112**, 146602 (2014).
[19] M. Nakamura, F. Kagawa, T. Tanigaki, H. S. Park, T. Matsuda, D. Shindo, Y. Tokura, and M. Kawasaki, Phys. Rev. Lett. **116**, 156801 (2016).
[20] M. Holtz, C. Hauf, A.-A. Hernández Salvador, R. Costard, M. Woerner, and T. Elsaesser, Phys. Rev. B **94**, 104302 (2016).
[21] M. Nakamura, S. Horiuchi, F. Kagawa, N. Ogawa, T. Kurumaji, Y. Tokura, and M. Kawasaki, Nature Communication **8**, 281 (2017).
[22] N. Ogawa, M. Sotome, Y. Kaneko, M. Ogino, and Y. Tokura, Phys. Rev. B **96**, 241203 (2017).
[23] K. Kushnir, Y. Qin, Y. Shen, G. Li, B. M. Fregoso, S. Tongay, and L. V. Titova, ACS Applied Materials & Interfaces **11**, 5492 (2019).
[24] D. Côté, N. Laman, and H. M. van Driel, Applied Physics Letters **80**, 905 (2002).
[25] A. Ghalgaoui, K. Reimann, M. Woerner, T. Elsaesser, C. Flytzanis, and K. Biermann, Phys. Rev. Lett. **121**, 266602 (2018).
[26] N. Laman, A. I. Shkrebtii, J. E. Sipe, and H. M. van Driel, Applied Physics Letters **75**, 2581 (1999).
[27] N. Laman, M. Bieler, and H. M. van Driel, Journal of Applied Physics **98**, 103507 (2005).
[28] M. Bieler, N. Laman, H. M. van Driel, and A. L. Smirl, Applied Physics Letters **86**, 061102 (2005).
[29] M. Bieler, K. Pierz, U. Siegner, and P. Dawson, Phys. Rev. B **76**, 161304 (2007).
[30] D. Rees, K. Manna, B. Lu, T. Morimoto, H. Borrmann, C. Felser, J. Moore, D. H. Torchinsky, and J. Orenstein, "Quantized photocurrents in the chiral multifold fermion system rhsi," ArXiv:1902.03230 [cond-mat.mes-hall].
[31] A. M. Burger, R. Agarwal, A. Aprelev, E. Schruba, A. Gutierrez-Perez, V. M. Fridkin, and J. E. Spanier, Science Advances **5** (2019).
[32] H. M. van Driel and J. E. Sipe, "Coherence control of photocurrents in semiconductors," (Springer, New York, NY, 2001) Chap. 5, pp. 261–306.
[33] J. Rioux and J. Sipe, Physica E: Low-dimensional Systems and Nanostructures **45**, 1 (2012).
[34] L. Z. Tan, F. Zheng, S. M. Young, F. Wang, S. Liu, and A. M. Rappe, npj Comput. Mater. **2**, 16026 (2016).
[35] R. D. King-Smith and D. Vanderbilt, Phys. Rev. B **47**, 1651 (1993).
[36] R. Resta, Rev. Mod. Phys. (1994).
[37] In the standard notation of susceptibilities[38] a permittivity of free space, ϵ_0, is factored out of χ_n. For clarity of notation we dont factor this term.
[38] R. W. Boyd, *Nonlinear Optics* (Academic Press; 2nd edition, San Diego, USA, 2003).
[39] C. Aversa and J. E. Sipe, Phys. Rev. B **52**, 14636 (1995).
[40] B. M. Fregoso, R. A. Muniz, and J. E. Sipe, Phys. Rev. Lett. **121**, 176604 (2018).
[41] C. Aversa and J. E. Sipe, IEEE Journal of Quantum Electronics **32**, 1570 (1996).
[42] D. E. Aspnes, Phys. Rev. B **6**, 4648 (1972).
[43] D. Culcer, A. Sekine, and A. H. MacDonald, Phys. Rev. B **96**, 035106 (2017).
[44] M. Bass, P. A. Franken, J. F. Ward, and G. Weinreich, Phys. Rev. Lett. **9**, 446 (1962).
[45] F. Nastos and J. E. Sipe, Phys. Rev. B **82**, 235204 (2010).
[46] P. U. Jepsen, R. H. Jacobsen, and S. R. Keiding, J. Opt. Soc. Am. B **13**, 2424 (1996).
[47] G. Li, K. Kushnir, M. Wang, Y. Dong, S. Chertopalov, A. M. Rao, V. N. Mochalin, R. Podila, K. Koski, and L. V. Titova, in *2018 43rd International Conference on Infrared, Millimeter, and Terahertz Waves (IRMMW-THz)* (2018).
[48] E. I. Blount, *Solid State Physics: Advances in Research and Applications*, Vol. vol 13 (Academic Press, 1962).
[49] F. D. M. Haldane, Phys. Rev. Lett. **93**, 206602 (2004).
[50] B.M. Fregoso unpublished.
[51] I. Sodemann and L. Fu, Phys. Rev. Lett. **115**, 216806 (2015).
[52] J. E. Moore and J. Orenstein, Phys. Rev. Lett. **105**, 026805 (2010).
[53] D. Xiao, M.-C. Chang, and Q. Niu, Rev. Mod. Phys. **82**, 1959 (2010).
[54] D. J. Thouless, M. Kohmoto, M. P. Nightingale, and M. den Nijs, Phys. Rev. Lett. **49**, 405 (1982).
[55] L. C. Gomes and A. Carvalho, Phys. Rev. B (2015).
[56] A. M. Cook, B. M. Fregoso, F. de Juan, S. Coh, and J. E. Moore, Nature Communications **8**, 14176 (2017).
[57] S. R. Panday and B. M. Fregoso, Journal of Physics: Condensed Matter **29**, 43LT01 (2017).

[58] H. Wang and X. Qian, Nano Letters **17**, 5027 (2017).
[59] S. R. Panday, S. Barraza-Lopez, T. Rangel, and B. M. Fregoso, "Injection current in ferroelectric group-iv monochalcogenide monolayers," ArXiv:1811.06474 [cond-mat.mes-hall].
[60] D. Sun, C. Divin, J. Rioux, J. E. Sipe, C. Berger, W. A. de Heer, P. N. First, and T. B. Norris, Nano Letters **10**, 1293 (2010).
[61] D. A. Bas, K. Vargas-Velez, S. Babakiray, T. A. Johnson, P. Borisov, T. D. Stanescu, D. Lederman, and A. D. Bristow, Applied Physics Letters **106**, 041109 (2015).
[62] D. A. Bas, R. A. Muniz, S. Babakiray, D. Lederman, J. E. Sipe, and A. D. Bristow, Opt. Express **24**, 23583 (2016).
[63] R. Atanasov, A. Haché, J. L. P. Hughes, H. M. van Driel, and J. E. Sipe, Phys. Rev. Lett. **76**, 1703 (1996).